# Potent and Selective *In Vitro* and *In Vivo* Antiproliferative Effects of Metal-Organic Trefoil Knots

*Farah Benyettou, Thirumurugan Prakasam, Anjana Ramdas Nair, Ini-Isabee Witzel, Marwa Alhashimi, Tina Skorjanc, John-Carl Olsen, Kirsten Sadler Edepli, and Ali Trabolsi**

## 1. General Materials and Methods

All reagents and starting materials were purchased from Sigma-Aldrich and used without further purification. The zinc trefoil knot, cadmium trefoil knot, diamino bipyridine (DAB) ligand and 2,6-diformyl pyridine were synthesized as previously reported.[1-3] Thin-layer chromatography (TLC) was performed on silica gel 60 F254 (E. Merck). The plates were inspected with UV light. Column chromatography was performed on silica gel 60F (Merck 9385, 0.040–0.063 mm). Routine nuclear magnetic resonance (NMR) spectra were recorded at 25 °C on a Bruker Advance III spectrometer, with working frequencies of 600 and 500 MHz for $^{1}H$, and 151.0 and 125.0 MHz for $^{13}C$ nuclei. All chemical shifts are reported in ppm relative to the signals corresponding to the residual non-deuterated solvents ($CD_3CN$: $\delta$= 1.94 ppm, $CD_3OD$: $\delta$= 3.31 ppm).[4, 5] All $^{13}C$ spectra were recorded with the simultaneous decoupling of proton nuclei. Coupling constant values (*J*) are given in hertz (Hz). The multiplicity of the proton spectrum is abbreviated in the following way: s (singlet), d (doublet), dd (doublet of doublets), t (triplet), q (quartet), qt (quintet), sx (sextet), m (multiplet) and a wide signal is preceded by br (broad). High resolution mass spectrometry (HRMS) analyses were performed using an Agilent 6540 UHA Accurate Mass Q-TOF / LC - MS-spectrometer in the positive mode and an acetonitrile/water used a gradient in C18 column. Phase contrast and fluorescence images were obtained on an Olympus FV1000MPE confocal scanning microscope. Optical

images were obtained on a DMI6000 Leica microscope. Flow cytometry experiments were performed on an Accuri C6 Flow Cytometer.

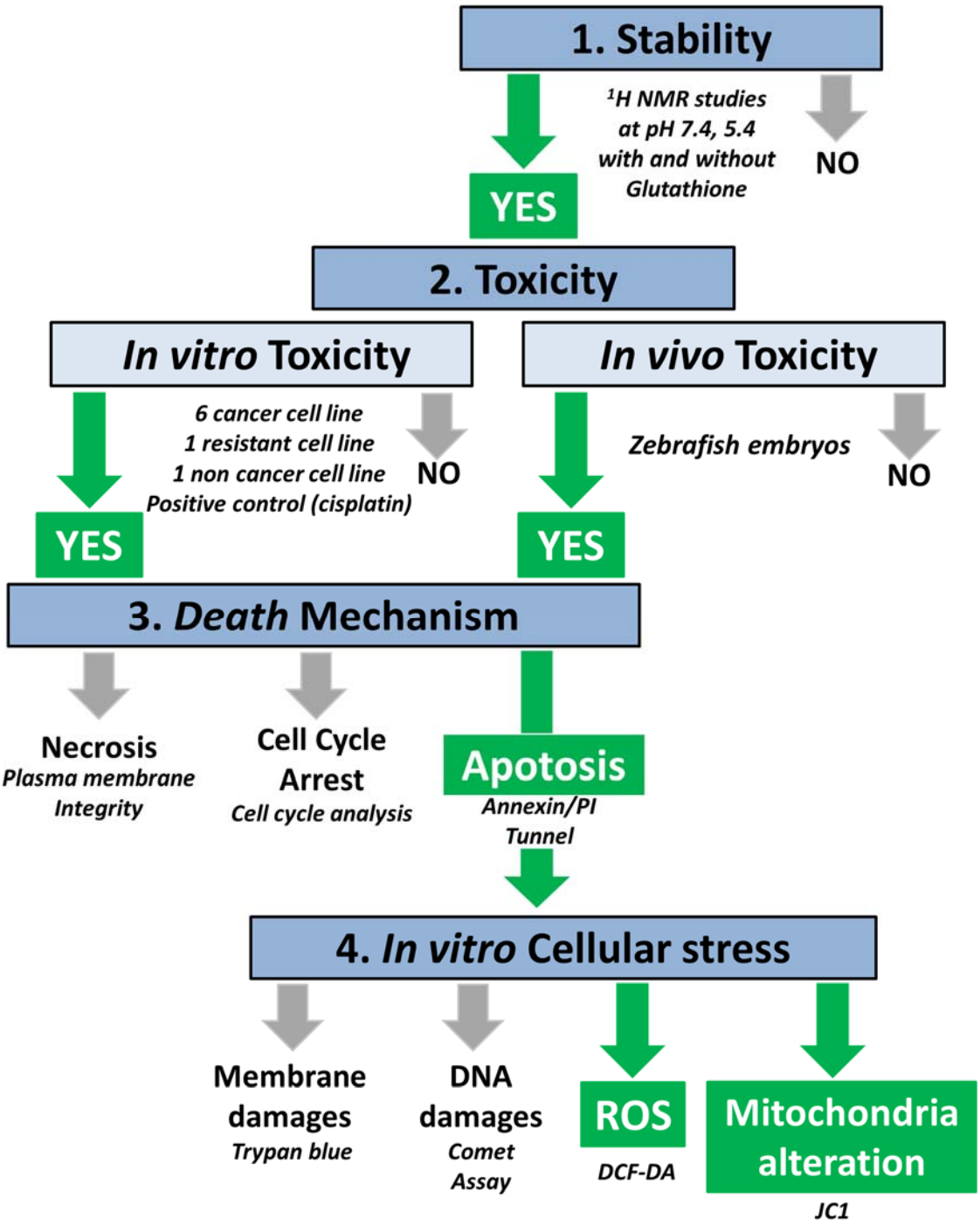


**Scheme S1.** Schematic representation of the logic of our study as well the step by step procedure we followed to systematically assess our compounds.

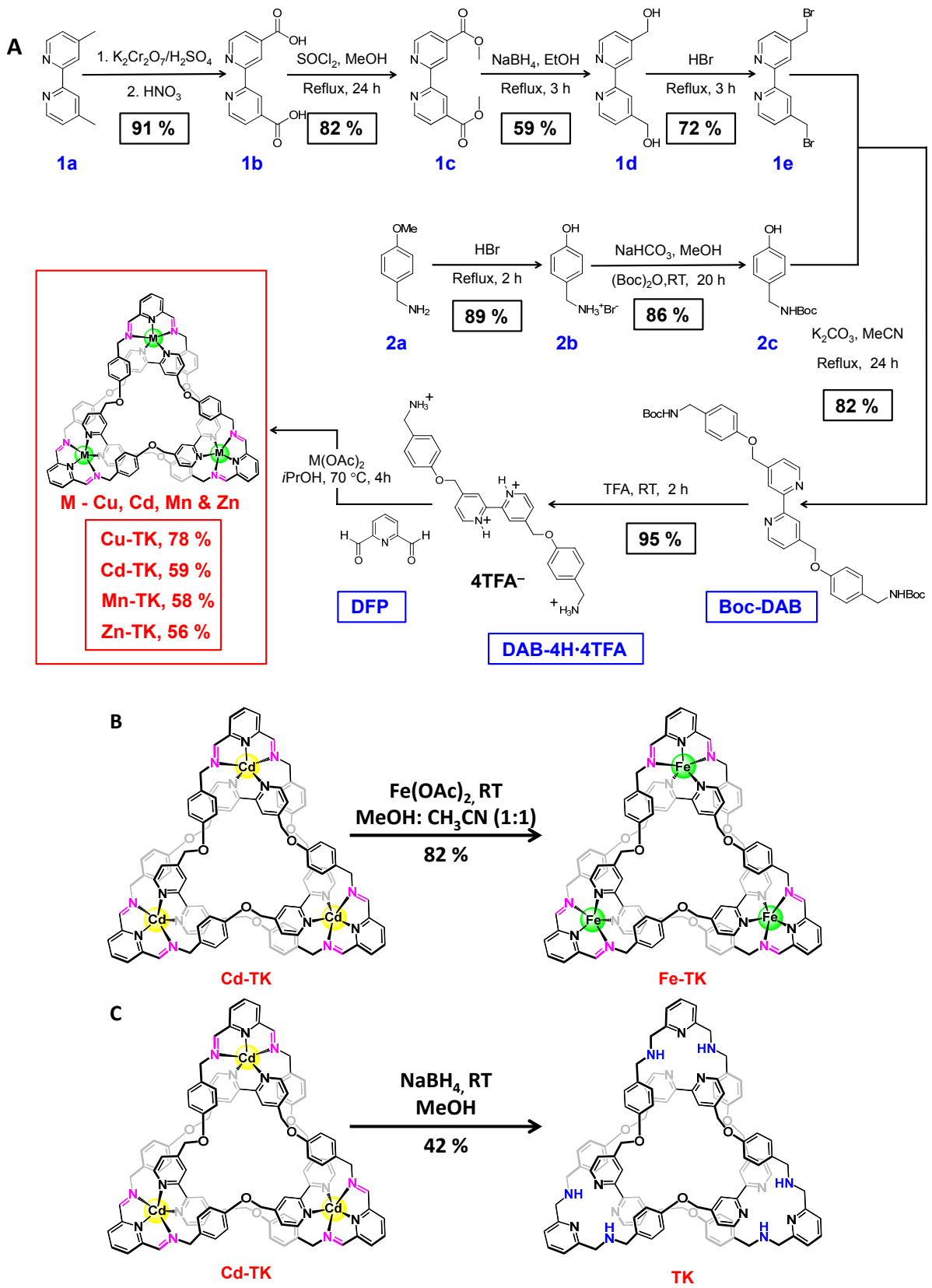


**Figure S1**. (A) Synthetic route for the formation of zinc(II), copper(II), manganese(II) and cadmium(II) metal templated trefoil knots from a simple pair of the ligands: trifluoroacetate

salt of diamino bipyridine and 2,6-diformyl pyridine and metal (II) acetate salt; (B) Transmetalation of Cd-TK yielded Fe-TK using 10 equivalent of iron (II) acetate in methanol and acetonitrile (1:1) mixed solvent system at room temperature; (C) Reduction of Cd-TK yielded Fe-TK using 40 equivalent of sodium borohydride in methanol at room temperature.[3]

2. General Synthetic Procedure

2.1. Making Metal Templated Trefoil Knots (M-TK)

Pale pink solid of freshly boc deprotected DAB·4TFA (0.21 mg, 0.25 mmol) was stirred with metal acetate salt (0.25 mmol) and 2,6-diformyl pyridine (DFP) (0.034 mg, 0.25 mmol) in 10 mL of isopropanol in a 50 mL round bottom flask. The reaction was refluxed at 70 °C for 5 hours. The warm solution was filtered and the obtained precipitate was washed with isopropanol. The precipitate was dried under vacuum for 6 hours and was isolated and identified as the trefoil knot using high resolution mass spectroscopy.

Trefoil knot, Cu-TK•6TFA: Yield: 78 % (0.154 mg); MS (ESI-HRMS): m/z Calcd for $(C_{107}H_{81}Cu_3F_{12}N_{15}O_{14})^{2+}$: 1108.1903 $[Cu\text{-}TK\bullet 4TFA]^{2+}$, found: 1108.1891 $[Cu\text{-}TK\bullet 4TFA]^{2+}$, m/z Calcd for $(C_{105}H_{81}Cu_3F_9N_{15}O_{12})^{3+}$: 703.1316 $[Cu\text{-}TK\bullet 3TFA]^{3+}$, found: 701.1311 $[Cu\text{-}TK\bullet 3TFA]^{3+}$, m/z Calcd for $(C_{103}H_{81}Cu_3F_6N_{15}O_{10})^{4+}$: 497.6023 $[Cu\text{-}TK\bullet 2TFA]^{4+}$, found: 497.6027 $[Cu\text{-}TK\bullet 2TFA]^{4+}$.

Trefoil knot, Mn-TK•6TFA: Yield: 58 % (0.115 mg); MS (ESI-HRMS): m/z Calcd for $(C_{107}H_{81}F_{12}Mn_3N_{15}O_{14})^{2+}$: 1096.202 $[Mn\text{-}TK\bullet 4TFA]^{2+}$, found: 1096.200 $[Mn\text{-}TK\bullet 4TFA]^{2+}$, m/z Calcd for $(C_{105}H_{81}F_9Mn_3N_{15}O_{12})^{3+}$: 693.139 $[Mn\text{-}TK\bullet 3TFA]^{3+}$, found: 693.138 $[Mn\text{-}TK\bullet 3TFA]^{3+}$, m/z Calcd for $(C_{103}H_{81}F_6Mn_3N_{15}O_{10})^{4+}$: 491.609 $[Mn\text{-}TK\bullet 2TFA]^{4+}$, found: 491.609 $[Mn\text{-}TK\bullet 2TFA]^{4+}$.

.

2.2. Transmetalation of Cd-TK with $Fe(OAc)_2$

Cd-TK.6TFA (25 mg, 9.6 µmol, 1 equiv.) was added to 10 equivalence of iron (II) acetate (16.7 mg, 10 equiv.) in 5 ml of degassed methanol and acetonitrile (1:1) mixture. The reaction mixture was stirred under argon atmosphere at room temperature for 3 h. After reaction completion, the mixture was concentrated in a rotary evaporator. To remove unwanted side products and excess iron (II) salts, the crude reaction mixture was washed with 10 mL thrice of isopropanol, and then, the reaction mixture was filtered. The obtained pink color solid was dried under vacuum for 15 h yielded 18.1 mg of pure iron(II) trefoil knot.

Trefoil knot, Fe-TK•6TFA: Yield: 82 %; $^1$H NMR (500MHz, MeOD-d4 and $CD_3CN$ (1:1), 25 °C): $\delta$ 4.67 (d, 12H, $J$ = 9.6, Hz,Ar-C$H_2$), 5.03 (brs, 12H, Ar-C$H_2$), 6.32 (d, 12H, $J$ = 7.4 Hz, Ar-$H$), 6.47 (d, 12H, $J$ = 7.3 Hz, Ar-$H$), 7.53 (brs, 6H, $J$ = 4.1 Hz, Ar-$H$), 8.19 (d, 6H, $J$ = 7.9 Hz, Ar-$H$), 8.49 (t, 3H, $J$ = 7.5 Hz, Ar-$H$), 8.83 (s, 6H, Ar-$H$), 9.21 (brs, 12H, Ar-$H$);$^{13}$C NMR (75 MHz, MeOD-d4, 25 °C): δ; 60.6, 67.5, 114.2, 119.0 (q, $^2J_{C\text{-}F}$ = 268 Hz, TFA), 120.9, 124.7, 129.1, 129.3, 129.9, 143.4, 147.4, 148.2, 148.9, 150.5, 157.0, 160.5, 163.4 (q, $^3J_{C\text{-}F}$ = 32 Hz. TFA); MS (ESI-HRMS): m/z Calcd for $(C_{107}H_{81}F_{12}N_{15}O_{14}Fe_3)^{2+}$: 1097.6966 [Fe-TK•4TFA]$^{2+}$, found: 1097.6943 [Fe-TK•4TFA]$^{2+}$, m/z Calcd for $(C_{105}H_{81}F_9N_{15}O_{12}\ Fe_3)^{3+}$: 694.1359 [Fe-TK•3TFA]$^{3+}$, found: 694.1339 [Fe-TK•3TFA]$^{3+}$.

Crystallographic characterization of Cu-TK

Detailed X-ray crystal structure determination data for Cu-TK are available in the Cambridge crystallography data center (CCDC), with the deposition number **CCDC 1549049.** All crystallographic data are available free of charge from the Cambridge Crystallographic Data Centre via www.ccdc.cam.ac.uk/data_request/cif

2.3. Stability of Zinc Trefoil Knot in Water

Deuterated aqueous solution of Zn-TK was prepared for checking their stability by NMR in physiological condition by adding 2.5 mg of Zn-TK in 0.6 mL of $D_2O$ to make a 1.7 mM of Zn-TK in the pH 7.4. After preparation of Zn-TK aqueous solution, a series of $^1H$ NMR spectrum was taken for Zn-TK at regular interval times namely 0 h, 6 h, 12 h, 24 h, 48 h, 60 h, 72 h and 96 h. The proton NMR spectra reveals that Zn-TK was stable up to 96h without any major degradation of the metal complexes as shown below figure. Favorable aqueous stability of Zn-TK probably arises from the presence of extensive (hydrophobic) pi-pi stacking of the Zn-TK metal complexes.

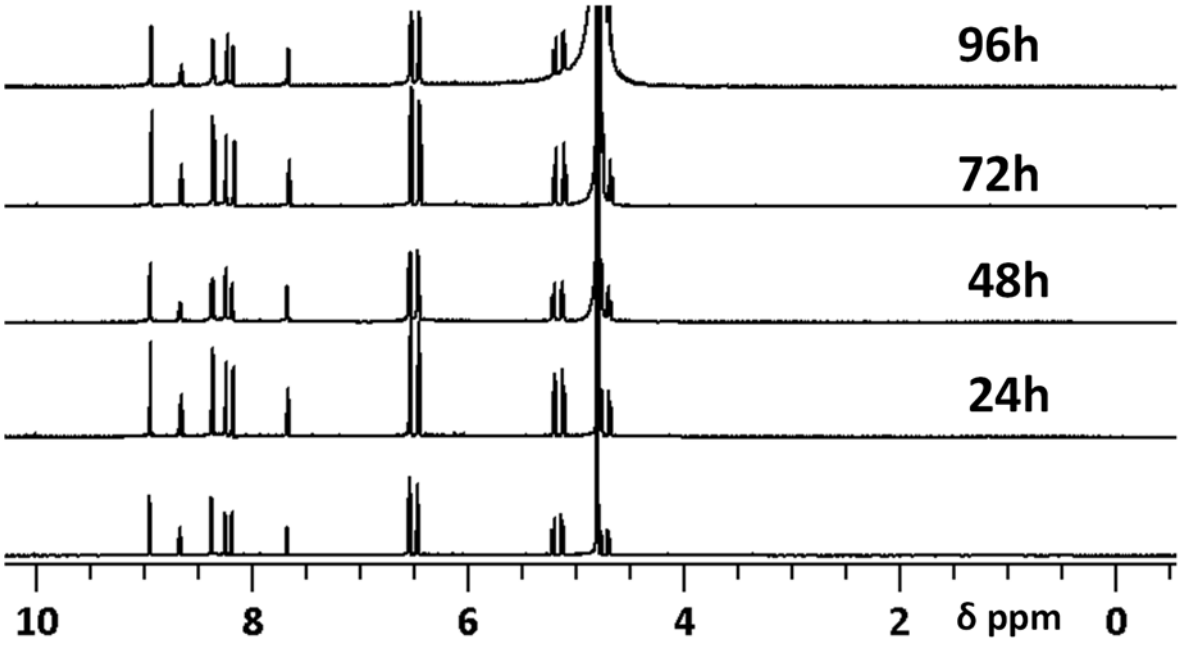


**Figure S2. Zn-TK are stable in water up to 4 days.** Stability of zinc trefoil knot in water was monitored by $^1H$ NMR spectroscopy. 0.6 mL of $D_2O$ solution of 1.7 mM Zn-TK. Bottom trace $^1H$ NMR spectrum of Zn-TK was recorded at room temperature when time = 0 and top trace $^1H$ NMR spectrum of Zn-TK recorded after 4 days.

2.4. Stability of zinc trefoil knot in glutathione

The interaction of Zn-TK (1.7 mM) with GSH (2 mM) in phosphate buffer solution was studied by $^{1}$H NMR at pH 7.4, in $D_2O$:DMSO (1:1). No distinct proton NMR spectral changes noticed when the $^{1}$H NMR spectra recorded for Zn-TK in the presence of glutathione in 1:1 ratio on comparison with spectra of Zn-TK in buffer solution and trend continued up to 96 h without any major decomposition of Zn-TK. As a result, formation of glutathione disulfide (GSSG) by oxidation of GSH was also not observed by $^{1}$H NMR (dH 3.30 ppm assignable to the b-$CH_2$ group of GSSG). The lack of spectral changes and the absence of GSSG formation indicate that the Zn-TK are stable against GSH reduction and might not induce GSH mediated resistance in cancer cells, unlike Cisplatin.

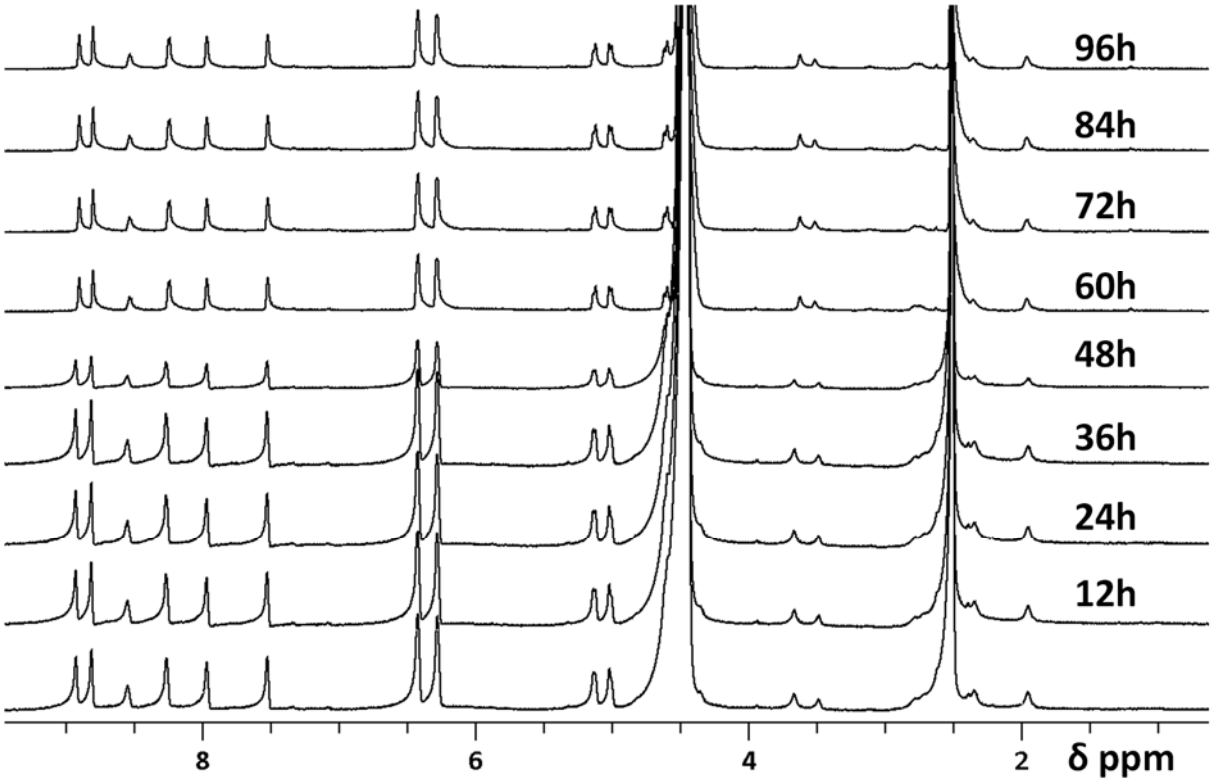


**Figure S3. Zn-TK are stable in presence of glutathione up to 4 days.** Stability of zinc trefoil knot in glutathione was monitored by $^{1}$H NMR spectroscopy. 1.7 mM of Zn-TK and glutathione used for checking the stability of zinc trefoil knot in $D_2O$ and DMSO (1:1) solvent mixture. Partial $^{1}$H NMR spectrum of 1.7 mM of Zn-TK and glutathione at pH 7 (bottom trace)

and after 96 h, $^{1}$H NMR spectrum of 1.7 mM of Zn-TK and glutathione at neutral pH 7. All reported spectra were recorded at 25 ºC in $D_2O$/DMSO-d6 (1:1) for solubility reason. The pH of glutathione solution was controlled by addition of dilute trifluoroacetic acid and fine adjustments were done by adding phosphate buffer solution.

2.5. Effect of pH on Zinc Trefoil Knot

The stability of Zn-TK was tested using $^{1}$H NMR spectroscopy at different pH in aqueous solution. 0.6 mL of 1.7 mM aqueous solution of Zn-TK were used to study effect of pH range 7.0 to below 5.5 in aqueous solution. The pH of Zn-TK solution lowered by titrating Zn-TK with dilute trifluoroacetic acid and fine adjustment of the pH. The corresponding effect of pH on Zn-TK shown below.

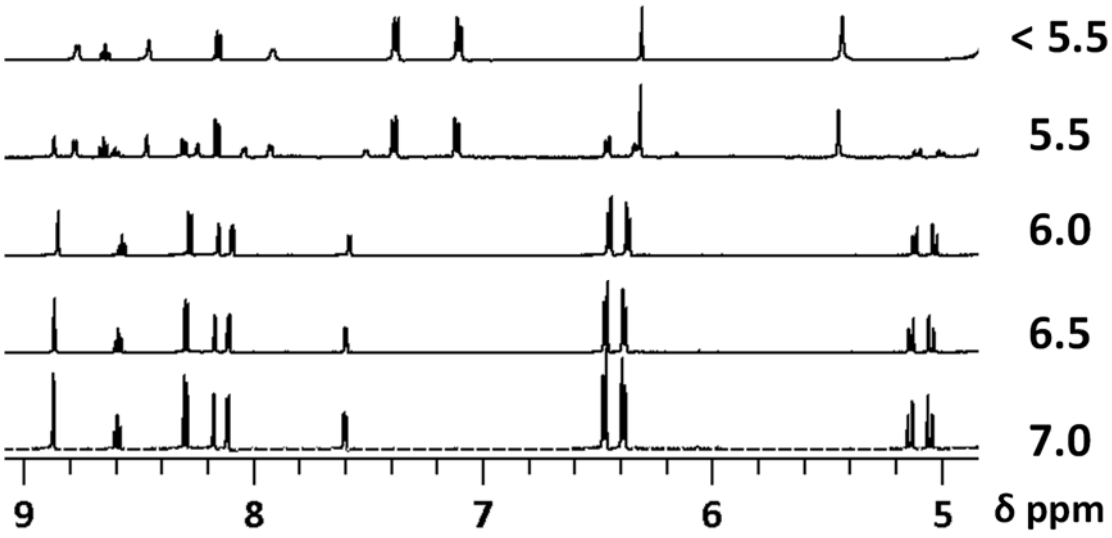


**Figure S4. Zn-TK are not stable in acidic conditions.** Stability of Zn-TK in solution at different pH was monitored by $^{1}$H NMR spectroscopy. Partial $^{1}$H NMR spectrum of 1.7 mM of Zn-TK at pH 7 (bottom trace) and decomposed knot at lower acidic pH (top trace). All reported spectra were recorded at 25 ºC in $H_2O/D_2O$. The pH of Zn-TK.6TFA solution was controlled by addition of dilute trifluoroacetic acid and fine adjustments were done by adding phosphate buffer solution.

3. Cell culture

Cervical epithelial cancer (HeLa; ATCC No. CCL-2), breast cancer (MCF-7, ATCC No.HTB-22; and MDAMB-231, ATCC No. HTB. 26), prostate cancer (PC-3; ATCC No. CRL1435), and non-cancer embryonic kidney 293 (HEK293; ATCC No. CRL-1573) cells were cultured at 5% $CO_2$ and 37 °C in Dulbecco's Modified Eagle's medium (DMEM) complemented with 10% fetal bovine serum (FBS) and 1 % penicillin/streptomycin. Ovarian cancer (A2780, ECACC 93112519) and cisplatin-resistant ovarian cancer cells (A2780/Cis, ECACC 93112517) were cultured at 5 % $CO_2$ and 37 °C in Roswell Park Memorial Institute (RPMI)-1640 medium complemented with 10 % fetal bovine serum (FBS) and 1% penicillin/streptomycin.

4. *In vitro* cell viability assay

Cell viability was assessed using CellTiter-Blue® Cell Viability assay (CTB, Promega). The assay measures the metabolic reduction of a non-fluorescent compound, resazurin, into a fluorescent product, resofurin, in living cells. As non-viable cells rapidly lose their metabolic activity, the amount of the resofurin product can be used to estimate the number of viable cells following treatment. Once produced, resofurin is released from living cells into the surrounding medium. Thus, the fluorescence intensity of the medium is proportional to the number of viable cells present.

96-well plates were seeded with cells (HeLa, MCF7, A2780, A2780/cis, MDAMB-231, PC3 and HEK-293) (~5,000 cells per well in 100µL of medium) and incubated at 37 °C for 24 hours. The medium was removed and replaced with fresh medium (control) or various concentrations of test compounds (up to 100 µM) and incubated at 37 °C for 48 hours. Thereafter, cells were incubated with 80 µL and 20 µL of CTB per well for 6 hours at 37 °C. The fluorescence of the resofurin product ($\lambda_{ex/em}$ 560/620) was measured. Untreated wells were used as control.

The percentage of cell viability and inhibition were calculated using the following formula:

$$\text{Viability (\%)} = [(F_{treated} - F_{blank}) / (F_{control} - F_{blank})] \times 100$$

$$\text{Inhibition (\%)} = 100 - \text{viability (\%)}$$

The $IC_{50}$ values were determined from a plot of percentage cell survival against drug concentration (in μM). All assays were conducted in triplicate and the mean $IC_{50}$ ± standard deviation was determined.

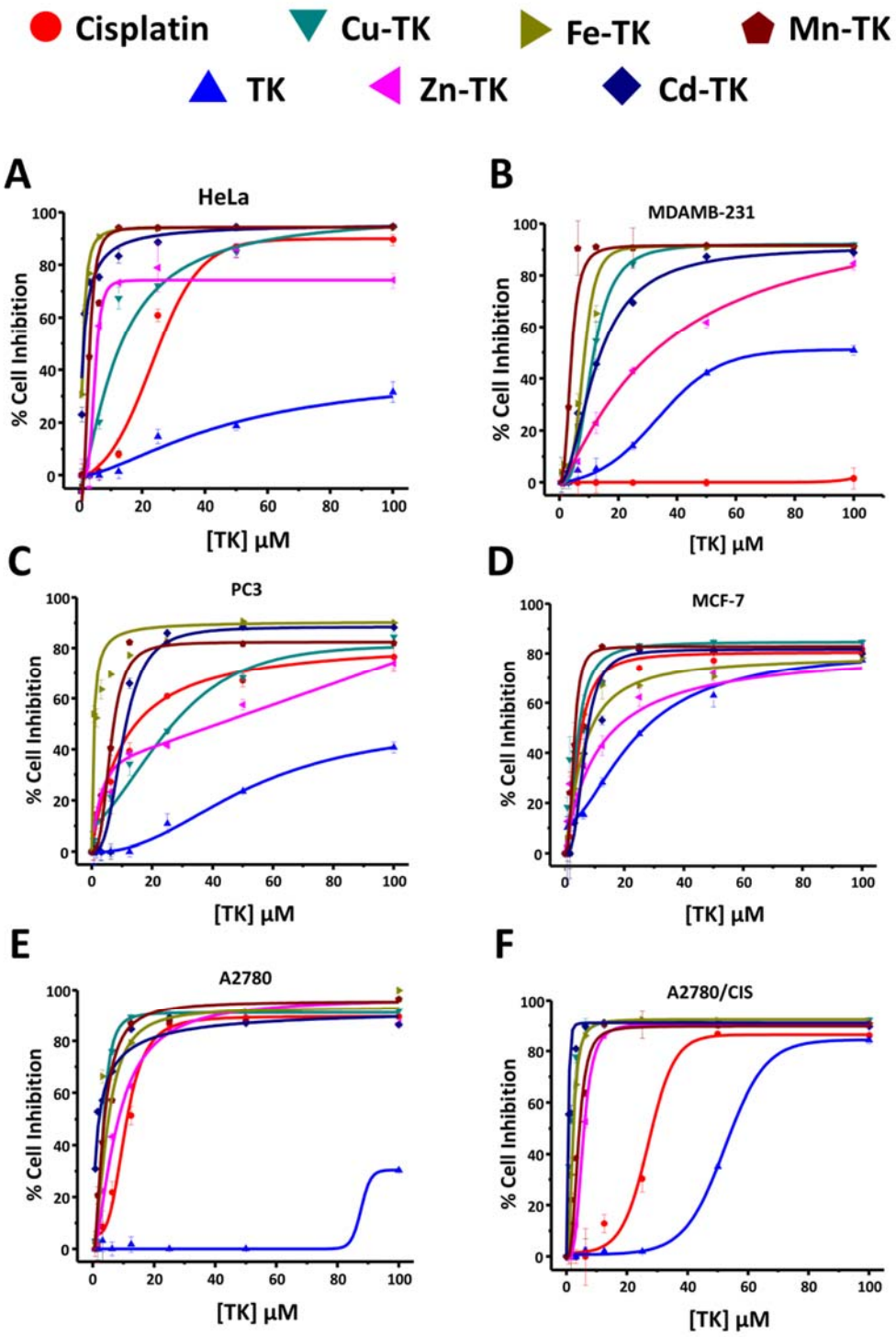


**Figure S5. M-TKs are toxic *In vitro* on cancer cells.** Cell Inhibition of A) HeLa, B) MDAMB-231, C) PC3, D) MCF-7, E) A2780 and F) A2780/CIS cells after 48 h incubation with test compounds. Red: cisplatin, blue: TK, green: Cu-TK, pink: Zn-TK, olive green: Fe-TK, dark blue: Cd-TK and maroon: Mn-TK. Error bars represent standard deviations of triplicate measurements.

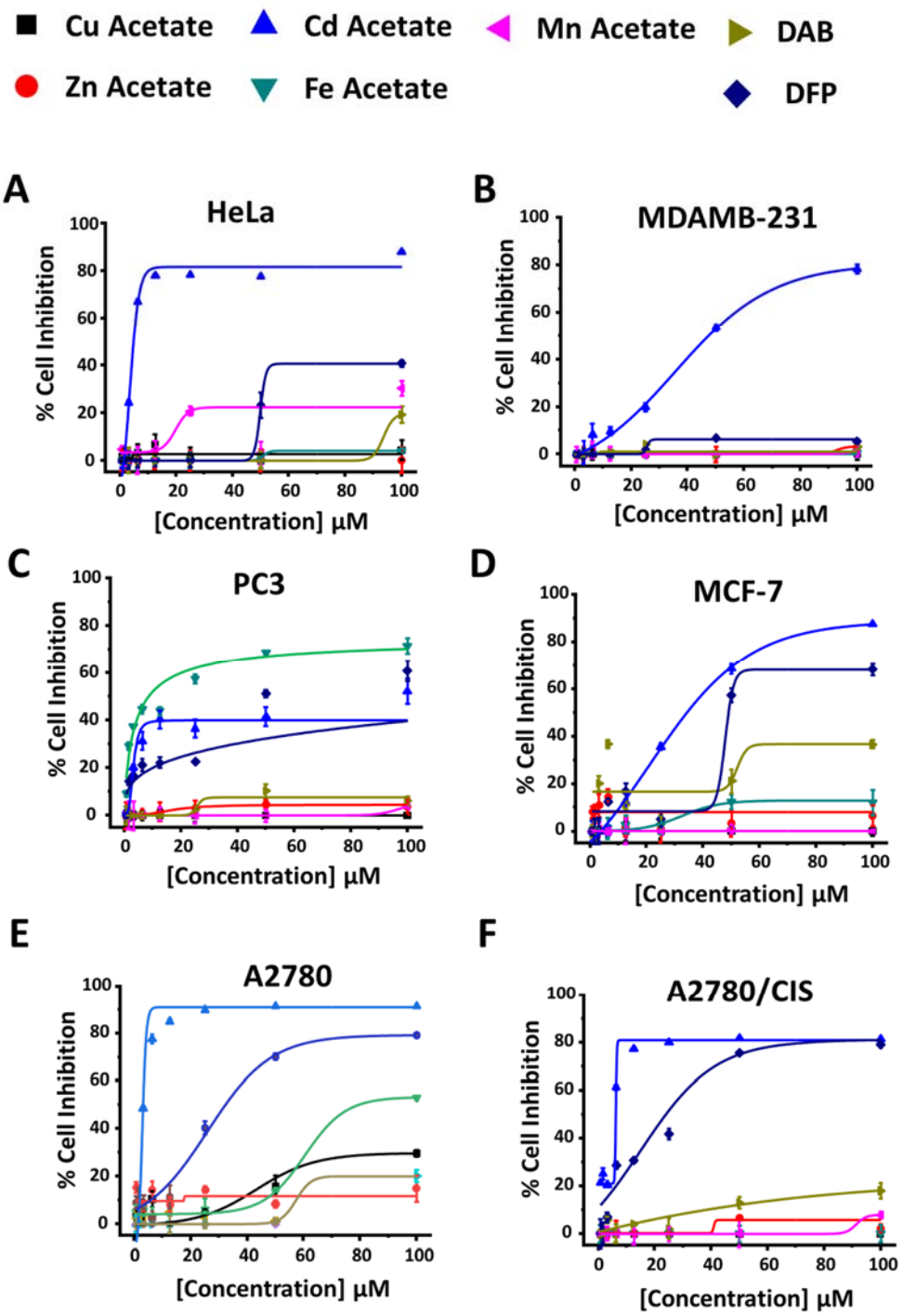


**Figure S6. Starting materials are overall less toxic on cancer cells than M-TKs.** Cell Inhibition of A) HeLa, B) MDAMB-231, C) PC3, D) MCF-7, E) A2780 and F) A2780/CIS cells after 48 h incubation with test compounds. Black: Cu-Acetate, blue: Cd-Acetate, red: Zn-Acetate, green: Fe-Acetate, pink: Mn-Acetate, olive green: DAB, dark blue: DFP. Error bars represent standard deviations of triplicate measurements.

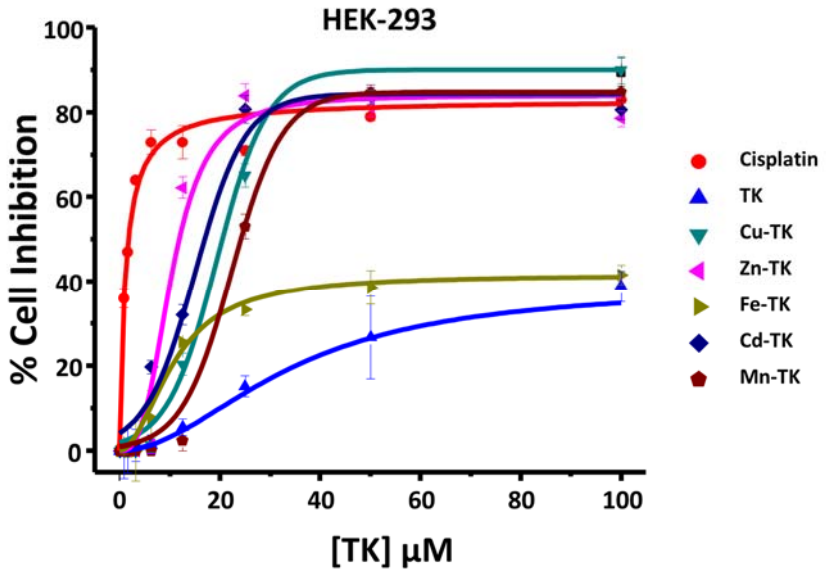


**Figure S7. M-TKs are less toxic than Cisplatin *In vitro* on non-cancer cells.** Cell Inhibition of HEK-293 cells after 48 h incubation with test compounds. Red: cisplatin, blue: TK, green: Cu-TK, pink: Zn-TK, olive green: Fe-TK, dark blue: Cd-TK and maroon: Mn-TK. Error bars represent standard deviations of triplicate measurements.

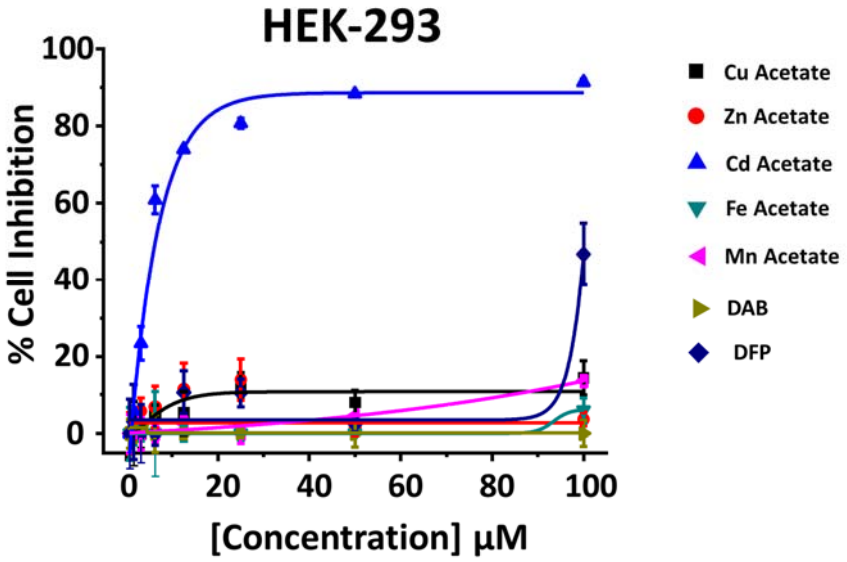


**Figure S8. Except Cd-Acetate, starting materials are not toxic on non-cancer cells.** *In vitro* toxicity assessment of starting materials. Cell Inhibition of HEK-293 cells after 48 h

incubation with test compounds. Black: Cu-Acetate, blue: Cd-Acetate, red: Zn-Acetate, green: Fe-Acetate, pink: Mn-Acetate, olive green: DAB, dark blue: DFP. Error bars represent standard deviations of triplicate measurements.

**Table S1.** Selective index (SI) and resistance factor (*Rf*) values of Cu-TK, Zn-TK, Fe-TK, Mn-TK, Cd-TK and Cisplatin against six cancer cell lines.

| | **SI** | | | | | | ***Rf*** |
|---|---|---|---|---|---|---|---|
| | **HeLa** | **A2780** | **A2780/cis** | **MDAMB** | **PC3** | **MCF-7** | |
| **Cu-TK** | 1.5 | 6.4 | 15.7 | 8.5 | 0.7 | 4.3 | *0.4* |
| **Zn-TK** | 2.2 | 1.4 | 2.1 | 2.0 | 0.3 | 0.7 | *0.7* |
| **Fe-TK** | 76.9 | 19.2 | 43.5 | 48.3 | 111.1 | 11.0 | *0.4* |
| **Cd-TK** | 11.2 | 8.0 | 28.1 | 8.8 | 1.4 | 2.2 | *0.3* |
| **Mn-TK** | 7.4 | 5.9 | 5.8 | 30.3 | 3.2 | 7.1 | *1.0* |
| **Cisplatin** | 0.1 | 0.2 | 0.1 | 0.1 | 0.1 | 0.3 | *2.5* |

5. *In vitro* Prussian blue staining to assess TK-Fe accumulation in cells

HeLa cells were seeded in 6-well plates in complete DMEM and incubated for 24 h. HeLa cells were treated with TK-Fe (2.5 μM, 24 h) and subsequently washed with PBS. HeLa cells were fixed with 70 % ethanol, washed with PBS, and stained with Perl's Prussian blue solution for 20 min at 37 °C with 5 % $CO_2$. Perl's Prussian blue solution was obtained by mixing in equal volumes 4 % potassium ferrocyanide solution and 4 % HCl. Staining (bright blue color) results from the reaction between the $Fe^{3+}$ ions present in the nanoparticles and the ferrocyanide ions. Cells were washed three times in PBS, the Prussian blue staining result was assessed under optical microscopy. The experiment was performed in triplicate.

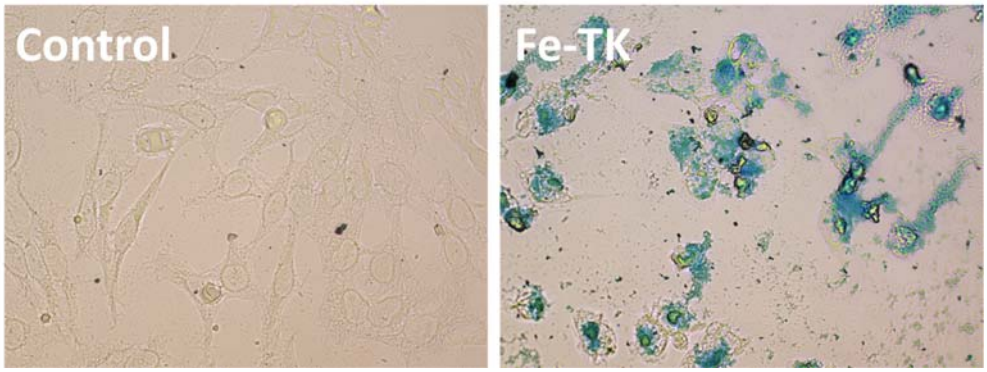


**Figure S9. Fe-TK penetrates HeLa cells.** Optical images of HeLa cells incubated with no additives (control) and with Fe-TK and stained using Prussian blue staining (2.5 µM, 24 h). (40 x magnification)

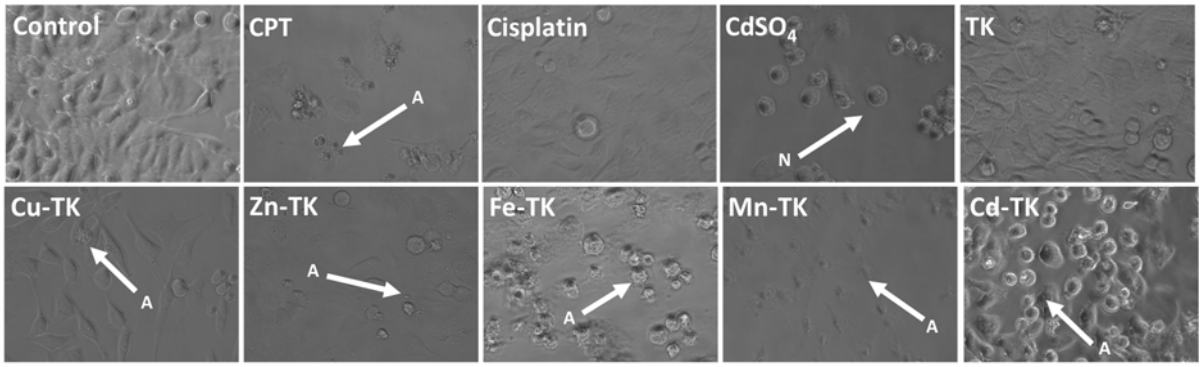


**Figure S10. HeLa cell morphology is altered after treatment with M-TKs.** Optical images of HeLa cells treated with no additives (control), or with CPT, cisplatin, $CdSO_4$, the metal-free TK, or the metal-based knots (Cu-TK, Zn-TK, Fe-TK, Mn-TK or Cd-TK), each at 10 µM for 24 hours. White arrows indicate apoptotic (A) and necrotic (N) bodies (20 x magnification). The experiment was performed in triplicate.

6. Cell membrane leakage study by the lactate dehydrogenase (LDH) assay.

HeLa cells were seeded in 96-well plates in complete DMEM at a density of $5.10^3$ cells/well and incubated for 24 h. HeLa cells were treated with test compounds (10 µM) for 3, 24 and 48 h. The LDH assay cell media supernatant was collected in a 96-well plate in triplicate

after treatment, and LDH reaction mixture was added to each well as recommended by the manufacturer's protocol (Thermo Fisher Scientific). After a 30-minute incubation at room temperature stop solution was added to each well and the absorbance at 490 and 680 nm of each well was determined using a plate reader. Percent LDH release was calculated and compared to untreated control cells.

7. Cell cycle analysis

To examine whether the growth inhibition observed resulted from cell cycle arrest or apoptosis, we examined the cell cycle distribution by staining treated HeLa cells with propidium iodide (PI) which stains DNA quantitatively and analyzed the proportion of cells in the various phases[6] – sub $G_1$ (apoptotic), $G_1$ (increase in size in readiness for DNA replication), S (DNA synthesis), $G_2$ (preparation for mitosis) and M (mitosis) by fluorescence *via* FACS analysis as a result of the differing amounts of DNA in the cells. The accumulation of cancer cells in particular phases of the cell cycle can point to the mode of action.

HeLa cells were seeded in 6-well plates in complete DMEM and incubated for 24 h, before test compound exposure (10 µM) for 24 h. HeLa cells were harvested and washed with PBS. Dead cells floating in the supernatant were also collected and washed with PBS. HeLa cells were fixed in 70 % ethanol for 1 h, at −20 °C. RNAse A (300 µl, 50 $\mu g.ml^{-1}$) was added to cells before incubation for 1 h following by the addition of a solution of propidium iodide (100 µl, 40 $\mu g.ml^{-1}$) in PBS in dark. Red fluorescence was observed at 488 nm excitation by flow cytometry to calculate percentages of cells in the Sub $G_0/G_1$, $G_0/G_1$, S and $G_2$/M phases. The assay was repeated three times with each compound. All values are expressed as mean ± STD. ($n = 3$). *$P < 0.05$, **$P < 0.01$ and ***$P < 0.001$ compared to the control.

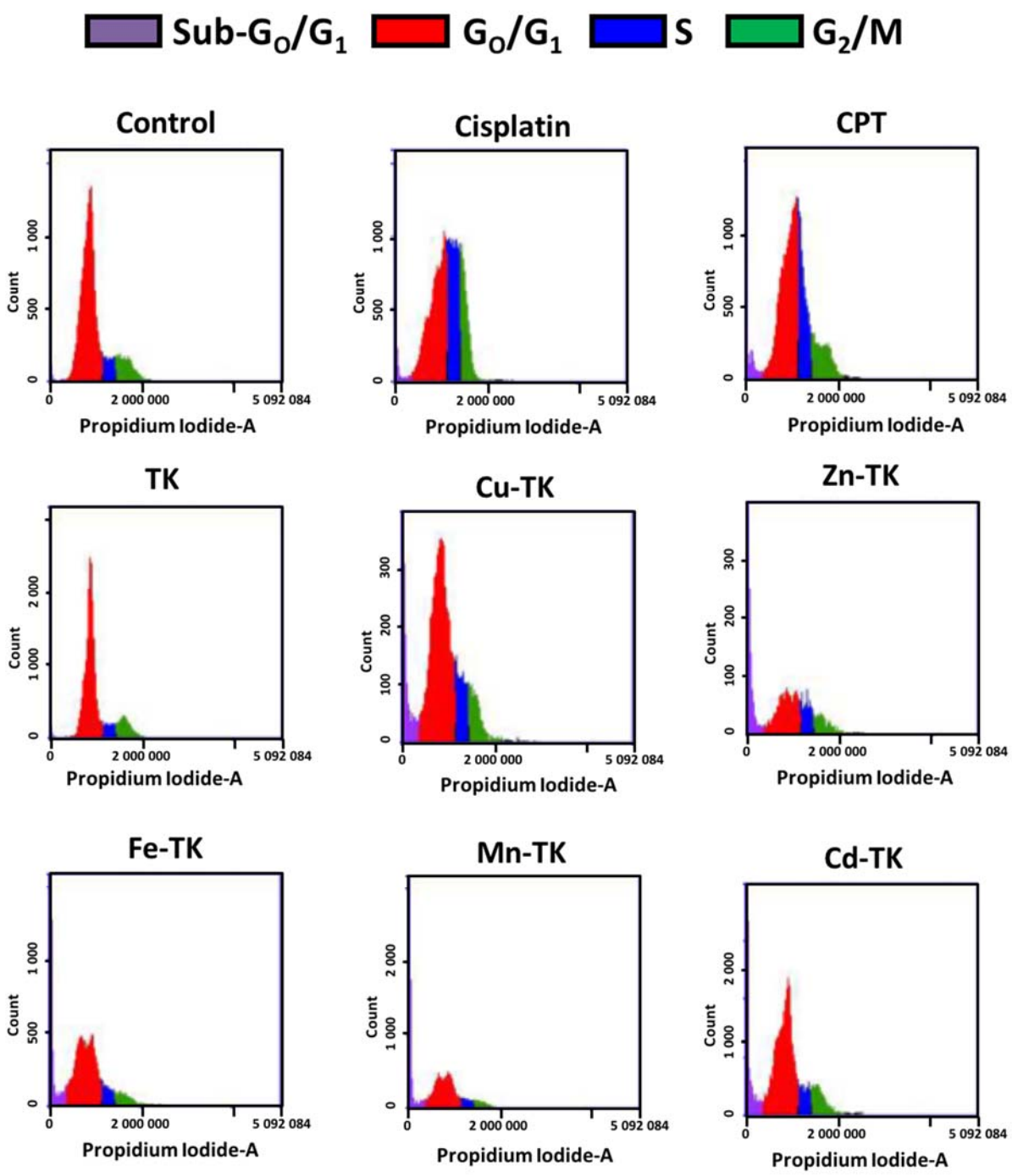


**Figure S11. M-TKs modify HeLa cell cycle.** Cell cycle analysis of HeLa cells treated with no additives (control), Cisplatin, CPT, TK, Cu-TK, Zn-TK, Fe-TK, Mn-TK and Cd-TK (10 μM) for 24 hours. The experiment was performed in triplicate.

8. Cell apoptosis detection using staining of Annexin V-FITC and PI

To further confirm whether the inhibition of cell growth was caused by apoptosis, we performed Annexin V-FITC /PI dual staining, followed by confocal microscopy and flow cytometric analysis. The translocation of phosphatidylserine (PS) from the inner leaflet to the outer leaflet of the plasma membrane is a marker of apoptosis. Apoptotic cells can be identified via fluorophore-labeled Annexin V-FITC, which has a high affinity for PS. In addition, PI nucleic acid dye gains entry into late apoptotic and necrotic cells, but not into early apoptotic and living cells. Therefore, various cell populations can be easily distinguished using Annexin V-FITC /PI dual staining.

HeLa cells apoptosis was studied using an Annexin V-fluorescein isothiocyanate (FITC) and propidium iodide (PI) apoptosis detection kit (BD Biosciences), according to the manufacturer's instruction. HeLa cells were seeded in 6-well plates in complete DMEM and incubated for 24 h, before test compound exposure (10 μM) for 24 h. HeLa cells were harvested and washed with PBS. Dead cells floating in the supernatant were also collected and washed with PBS. HeLa cells were incubated in binding buffer with FITC (10 μl, 100 $\mu g.ml^{-1}$) for 60 min and PI (5 μl, 100 $\mu g.ml^{-1}$) for 5 min in dark. Apoptotic cells were identified by flow cytometry and confocal microscopy. For confocal and fluorescence microscopy, same protocol was applied with addition of DAPI (5 μl, 100 $\mu g.ml^{-1}$) to stain nuclei. Each sample was assayed in duplicate, and the experiment was repeated 3 times.

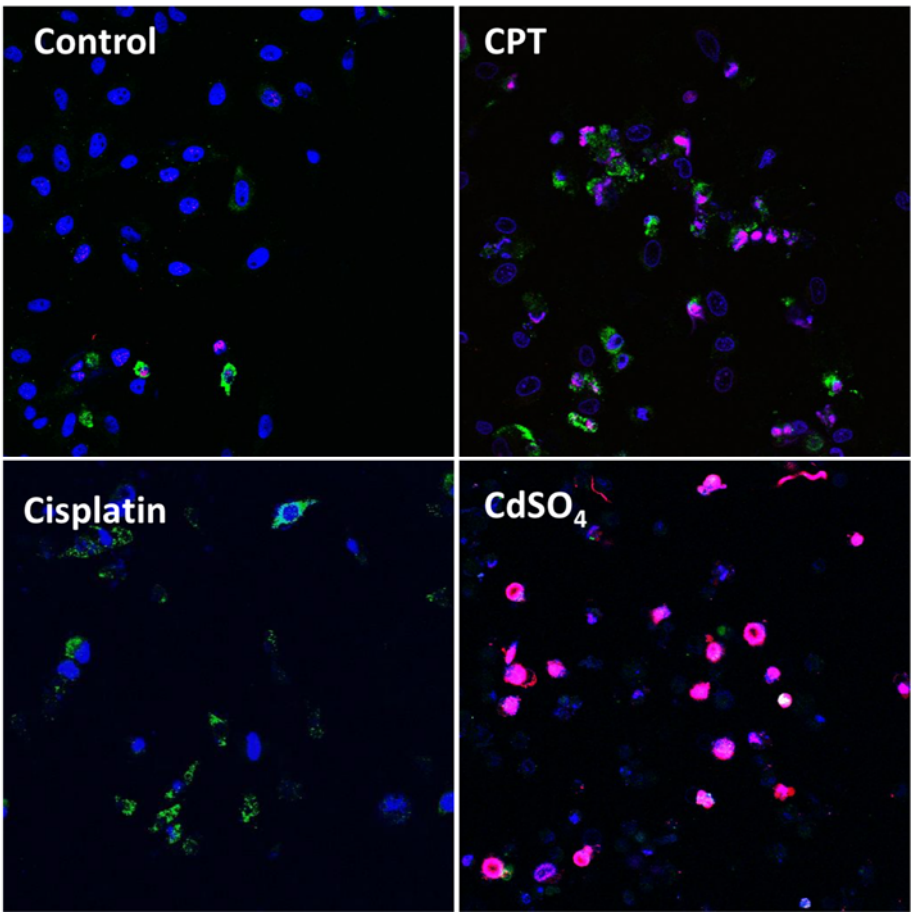


**Figure S12. CPT and Cisplatin induce apoptosis, while CdSO4 trigger necrosis.** Apoptosis observation after Annexin/PI staining in HeLa cells incubated for 3 hours with no additives (control) or with CPT, cisplatin or $CdSO_4$ (10 µM), followed by staining with Annexin V-FITC (green), DAPI (blue) and propidium iodide (red). DAPI staining was used as a nuclear marker.

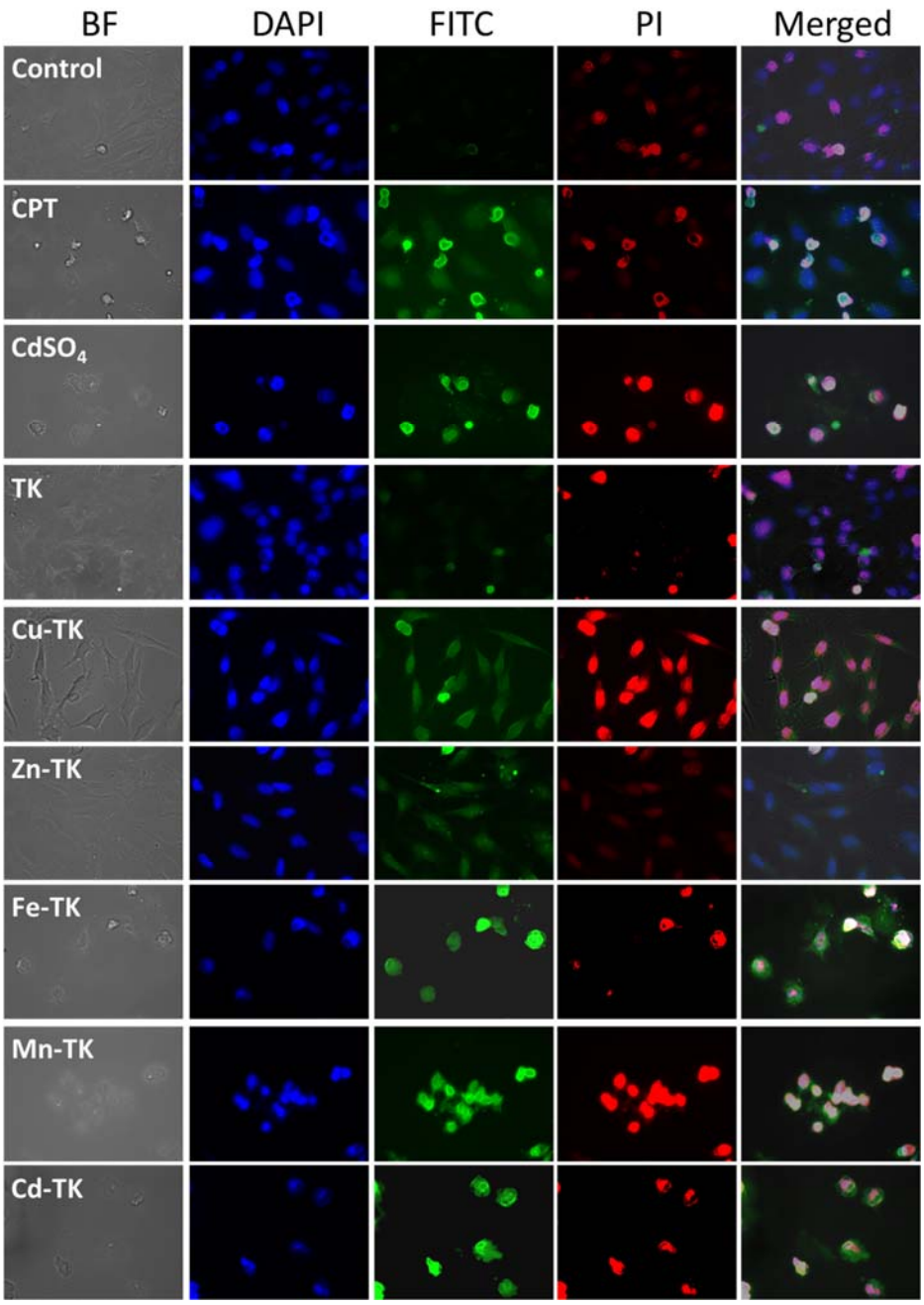


**Figure S13. M-TKs induce apoptosis in HeLa cells.** Bright field and fluorescence microscopy images of HeLa cells incubated with no additives (control), CPT, $CdSO_4$, TK, Cu-TK, Zn-TK, Fe-TK, Mn-TK and Cd-TK (10 μM) for 24 hours followed by incubation with DAPI (blue), Annexin V-FITC (green) and propidium Iodide (red). Both viable and nonviable cells nuclei are stained with DAPI. Treated cells that exerted apoptosis characteristics emitted bright green fluorescence, brighter blue fluorescence and bright red fluorescence after staining. The experiment was performed in triplicate.

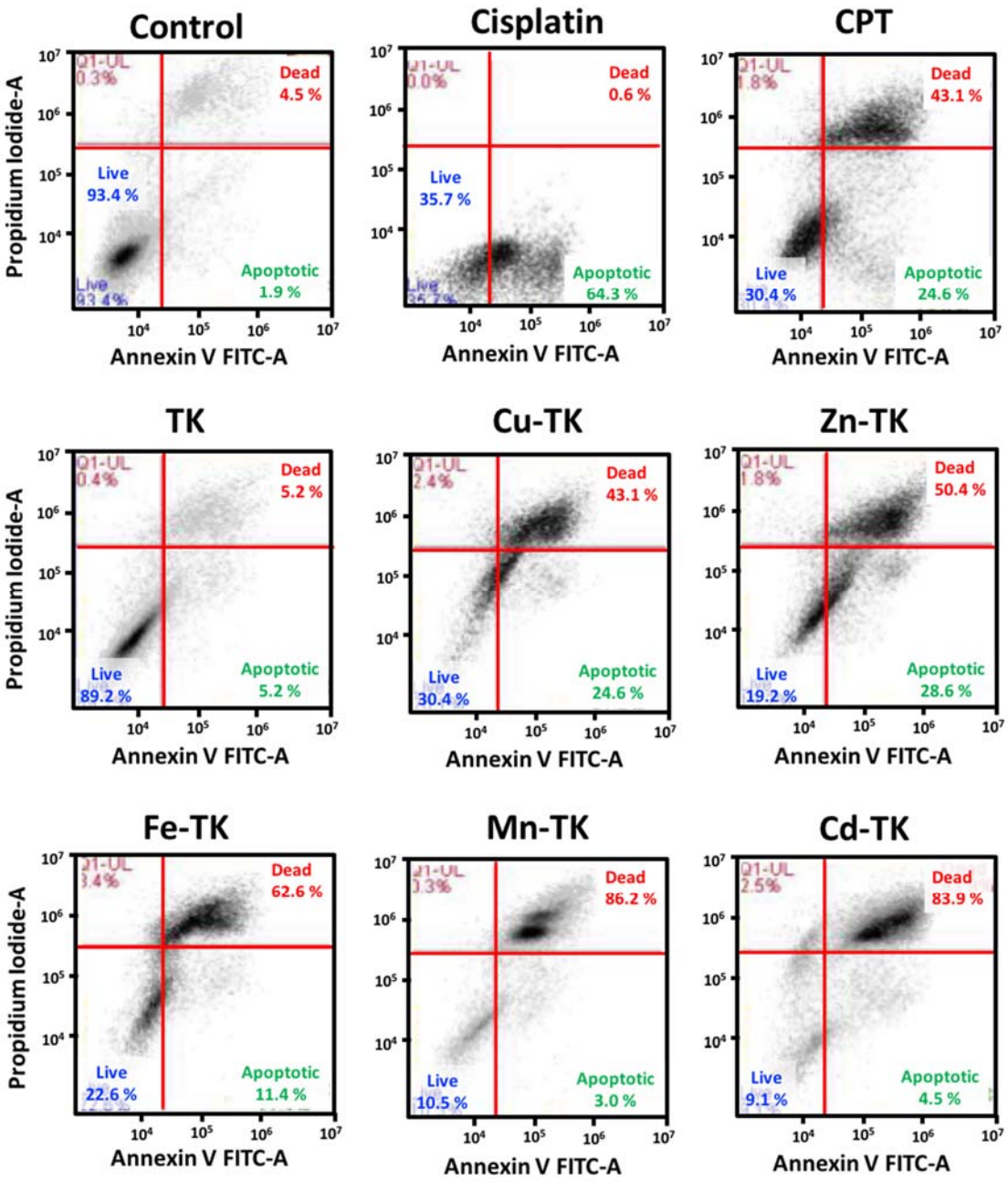


**Figure S14. M-TKs trigger high level of apoptosis in HeLa cells.** Effect of no additives (control), Cisplatin, CPT, TK, Cu-TK, Zn-TK, Fe-TK, Mn-TK and Cd-TK (10 μM) for 24 hours on apoptosis in HeLa cells using staining of Annexin V-FITC and PI. The cell distributions in flow cytometric histograms are as follow: cells in the lower left quadrant represented live cells, negative for Annexin V and PI; the lower right quadrant represented early apoptotic cells; the upper right quadrant represented late apoptotic cells; and upper left quadrant represent necrotic cells. The experiment was performed in triplicate.

9. Mechanism of cellular internalization and release in HeLa cells of Mn-TK using Annexin V-FITC and PI dual staining

| Endocytic Inhibitor | Pathway inhibited | Concentration (µM) |
|---|---|---|
| Chlorpromazin | Clathrin-mediated endocytosis | 5 |
| Methyl-B-Cyclodextrin (MBCD) | Lipid raft | 10 |
| Filipin | Clathrin-independant endocytosis | 5 |
| Amiloride | Macropinocytosis | 10 |
| Ammonium Chloride (AmCl) | Lysosome acidification | 50 |

**Table S2.** Concentrations of endocytic inhibitors used in this study.

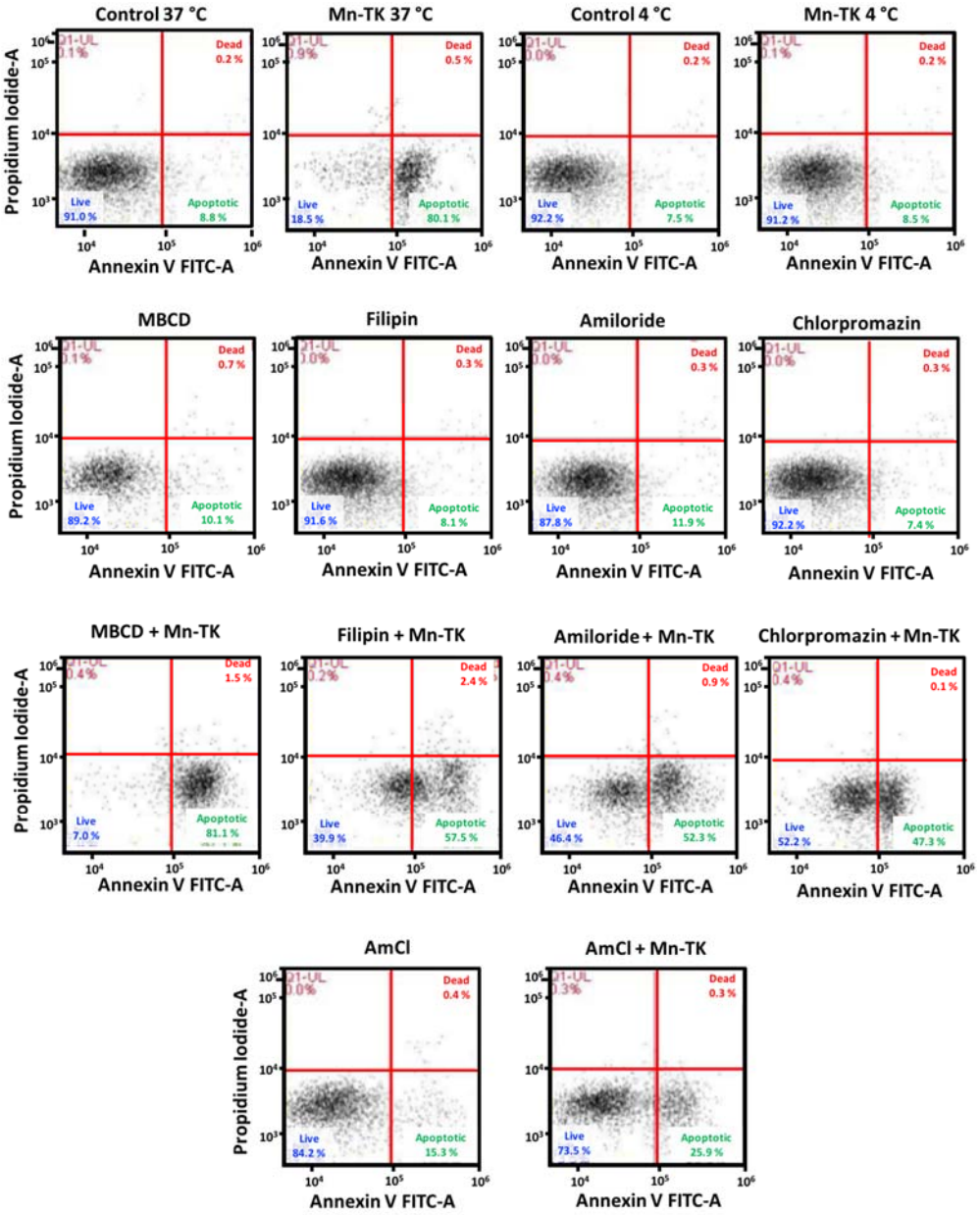


**Figure S15. M-TK penetrate into HeLa cell using endocytosis mechanisms.** Internalization mechanism study using Annexin/PI staining. Effect of incubation at 37 °C, 4 °C, endocytotic inhibitors (Chlorpromazin, Methyl-B-Cyclodextrin (MBCD), Filipin, Amiloride and Ammonium Chloride (AmCl)) on apoptosis of HeLa cells treated with Mn-TK (10 µM, 3 hours) and untreated cells using staining of Annexin V-FITC and PI. Apoptosis test were also performed with inhibitors alone in order to determine the concentration where they block the pathways without toxicity. Cell death was negligible for the concentrations used. The experiment was performed in triplicate.

10. Membrane integrity by trypan blue exclusion staining

Drugs that can disrupt the cell membrane by forming pores can cause cell apoptotic or necrotic death.[7, 8] We decided to study whether Metal-TK compounds are causing membrane damage as their primary mechanism to trigger apoptosis. For this purpose, we performed a dye-exclusion assay on treated HeLa cell, to assess cell membrane integrity. In a healthy cell, the intact membrane will prevent trypan blue dye from entering cells. In a damaged cell, trypan blue will enter the cell, staining it blue. Results were compared to cells treated with lysis buffer, which induces total membrane damage. Cell membrane damage % was deduced from comparing the number of stained cells induced by treatment with the number of stained cells after lysis.

HeLa cells were seeded in 6-well plates in complete DMEM and incubated for 24 h, then treated with test compounds (10 μM, 4 h), harvested and washed with PBS. Trypan blue (10 μL, 0.4 % in water) was added to the cells. The number of damaged cells stained in blue were counted and imaged using an optical microscope (DMI6000, Leica) within 5 minutes after dye addition. The assay was repeated three times with each compound. All values are expressed as mean ± STD. ($n = 3$). *$P < 0.05$, **$P < 0.01$ and ***$P < 0.001$ compared to the control.

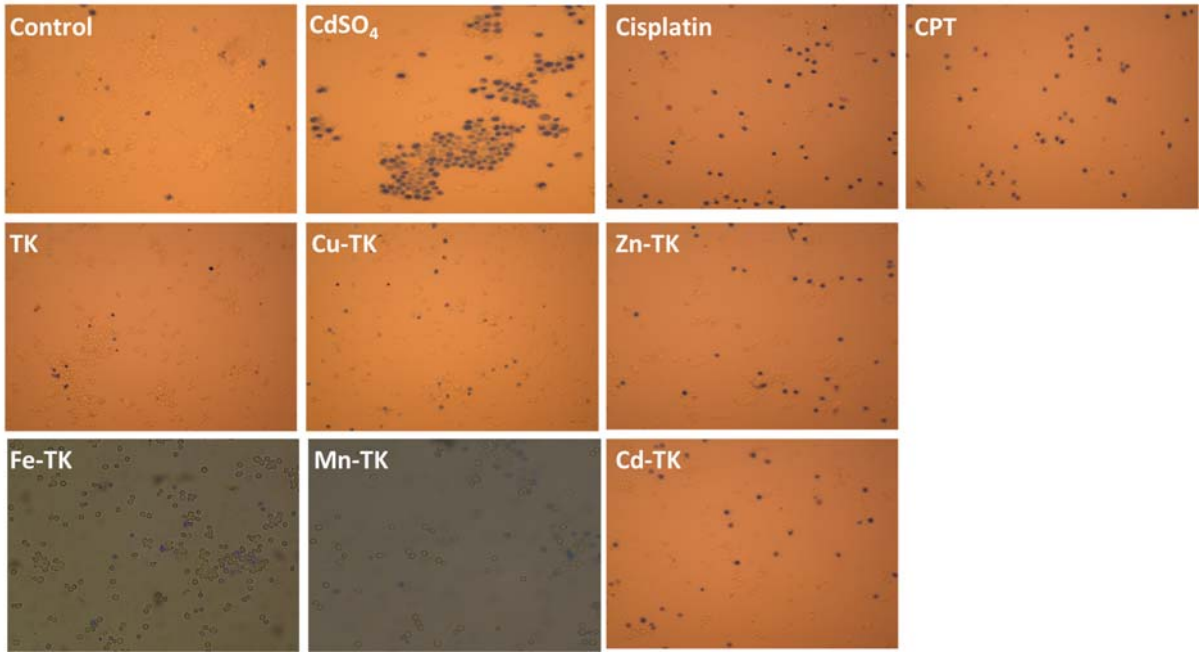


**Figure S16. M-TKs do not alter HeLa cell membrane integrity.** Cell membrane integrity remains intact after M-TK exposure. trypan blue exclusion staining of HeLa cells treated with CPT, Cisplatin, TK, Cu-TK, Zn-TK, Fe-TK, Mn-TK and Cd-TK (10 µM) for 3 hours, and untreated cells (control) after trypan blue exclusion staining. Quantification was based on counting individual cells clearly separated. (10 x magnification). The experiment was performed in triplicate.

11. Alkaline comet assays.

11.1. Classic Alkaline comet assay

HeLa cells were seeded in 6-well plates into complete DMEM and incubated for 24 h. Cells were treated with test compounds at 10 µM for 10 minutes and then washed, harvested, and embedded in a thin film of agarose on a glass slide. The slides were subjected to horizontal gel electrophoresis (16 V, 35 min) and then washed, dried, and stained with DAPI (2 $\mu g.ml^{-1}$). Images were taken using a fluorescent microscope (DMI6000, Leica) and the tail DNA % of comets (percentage of DNA in the tail vs the head of the comet) was analyzed using Fiji

software and the Open Comet plugin. Each experiment was carried out in triplicate, using biological replicates. Statistical analysis was performed using STATA SE14.2.

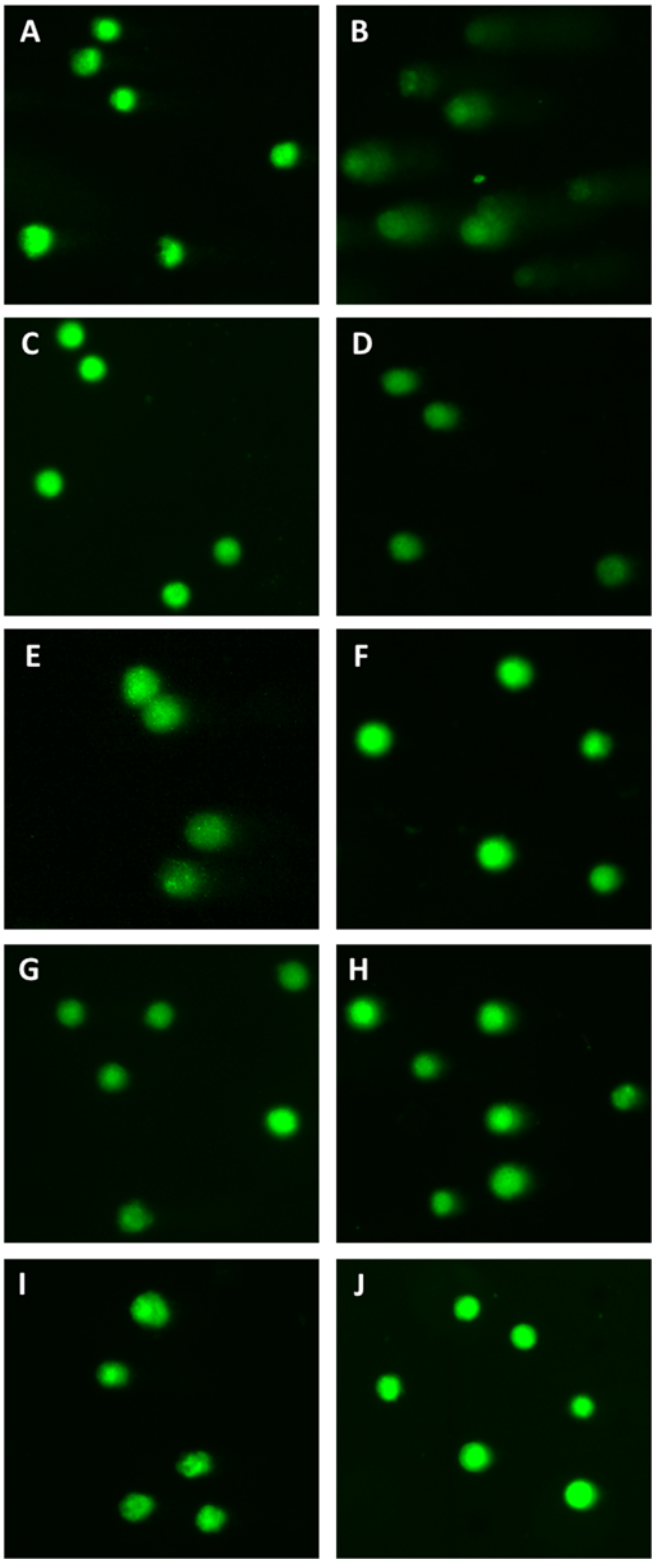

**Figure S17. DNA damage does not occur in HeLa cells treated with M-TKs.** The alkaline comet assay was used on cells either left untreated (Control, A), or treated with 10 μM $H_2O_2$ (B) for 2 min, or 10 μM cisplatin (C), CPT (D), TK (E), Cu-TK (F), Zn-TK (G), Fe-TK (H), Mn-TK (I) or Cd-TK (J) for 10 minutes. Images were analyzed using Fiji software and the OpenComet plugin, and treatments were compared based on their median % tail DNA. Results are representative of three biological replicates and no statistically significant difference was observed between control cells and cisplatin, CPT or M-TK treated cells (Anova, Bonferroni post-hoc, $p > 0.05$). A significant difference was only detected between control cells and $H_2O_2$-treated positive controls ($p < 0.005$).

11.2. Cross linking comet assay

To detect DNA crosslinking, HeLa cells were seeded as for the alkaline comet assay and incubated for 24 h. Cells were treated with test compounds at 5 μM and incubated overnight for 12 h. Cells underwent a 10-minute treatment with hydrogen peroxide (10 μM) prior to harvesting the cells for an alkaline comet assay, as described above. Tail DNA % of these cells was compared to cells that were not treated with hydrogen peroxide. Each experiment was carried out in triplicate, using biological replicates. Statistical analysis was performed using STATA SE14.2.

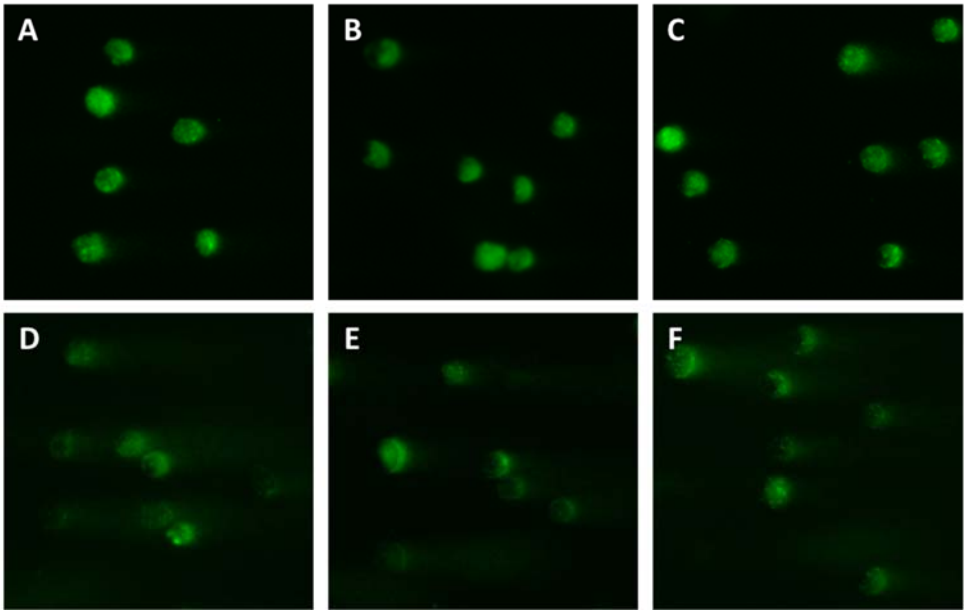


**Figure S18. DNA crosslinking does not occur in HeLa cells treated with M-TKs.** Investigation of the ability of Zn-TK to cause DNA crosslinking, by means of a crosslinking alkaline comet assay. HeLa cells were left untreated (Control, A), or treated with 10 μM cisplatin overnight (B) or 10 μM Zn-TK overnight (C). Following this 12-hour incubation, subsets of control cells (D), cisplatin-treated cells (E) and Zn-TK-treated cells (F) were also exposed to 10 μM $H_2O_2$ for 2 minutes. Fluorescent comet images were taken at 20x magnification and analyzed using Fiji software and the OpenComet plugin, to compare treatments on the basis of median % tail DNA. All $H_2O_2$-exposed cells showed the same extent of % tail DNA, with no significant decrease observed with cisplatin or Zn-TK treatments relative to the control-$H_2O_2$ cells (D), indicating no significant crosslinking (Anova, Bonferroni post-test, $p > 0.005$). Results are representative of three biological replicates.

12 – ROS generation

Reactive oxygen species (ROS) is produced especially when cells undergo chemical or environmental stress and could be one of the causative factors leading to cell cycle arrest or apoptosis.[9] Triggering apoptosis in cancer cells by generation of free radicals is the mechanism

of action of various chemotherapeutic drugs. To determine if treatment with Metal-TKs affected the level of ROS generation, the intracellular ROS level was identified using the fluorescent dye DCF-DA (2′,7′-dichlorodihydrofluorescein diacetate), which forms highly fluorescent DCF (2′,7′-dichlorofluorescein) in the presence of ROS. Flow cytometry was carried out to check the level of ROS generation. Results were compared to cells treated with $H_2O_2$ (100 μM) which induced maximum ROS generation and is considered as the 100 %. ROS % was calculated by comparing the ROS generation induced by treatment with ROS produced in cells treated with $H_2O_2$.

The level of intracellular ROS was measured *in situ* using flow cytometry in HeLa cells stained with $H_2$-DCFDA (2′,7′-dichlorodihydrofluorescein diacetate) fluorescent probes (Molecular Probes). HeLa cells were seeded in 6-well plates in complete DMEM and incubated for 24 h, before test compounds exposure (10 μM) for 3 h. HeLa cells were harvested and washed with PBS. Dead cells floating in the supernatant were also harvested and washed with PBS. The cells were suspended in PBS containing 10 μM of $H_2$-DCFDA. The cells were incubated for 30 min at 37 °C, washed twice with PBS and re-suspended in PBS. The fluorescence was measured using a flow cytometer. The level of ROS was estimated as a mean value of $H_2$-DCFDA fluorescence in $5.10^4$ cells. The assay was repeated three times with each compound. All values are expressed as mean ± STD. ($n = 3$). *$P < 0.05$, **$P < 0.01$ and ***$P < 0.001$ compared to the control.

13. Mitochondrial membrane potential ($\Delta\Psi m$) alterations

ROS hyper generation and oxidative stress is associated with disturbances in the mitochondrial membrane permeabilization, thus indicating the activation of the intrinsic apoptotic pathway. Determination of changes in mitochondrial permeability provide an early signal of the initiation of cellular apoptosis. We further examined the mitochondrial membrane potential ($\Delta\psi m$) using

the membrane-permeant JC-1 dye (5,5′,6,6′-tetraethyl-benzimidazolylcarbocyanine iodide) by flow cytometry. JC-1 forms aggregates with red fluorescence in healthy cells with intact mitochondria, but it shows monomeric green fluorescence in early apoptotic cells. Flow cytometry was carried out to assess the mitochondrial alteration.

The changes in mitochondrial transmembrane potential was measured *in situ* using flow cytometry in cells stained with the membrane potential-sensitive dye JC-1 (5,5′,6,6′-tetraethyl-benzimidazolylcarbocyanine iodide, Molecular Probes). HeLa cells were seeded in 6-well plates in complete DMEM and incubated for 24 h, before treatment exposure (10 µM) for 1 h. HeLa cells were harvested and washed with PBS. Dead cells floating in the supernatant were also harvested and washed with PBS. Cells were suspended in PBS containing JC-1 (10 $\mu g.ml^{-1}$) for 30 min at 37 °C, washed and re-suspended in PBS. Fluorescence was measured in $5.10^4$ cells using a flow cytometer, using a 488 nm laser for excitation and recording emission at 530/590 nm. The assay was repeated three times with each compound. All values are expressed as mean ± STD. ($n = 3$). *$P < 0.05$, **$P < 0.01$ and ***$P < 0.001$ compared to the control.

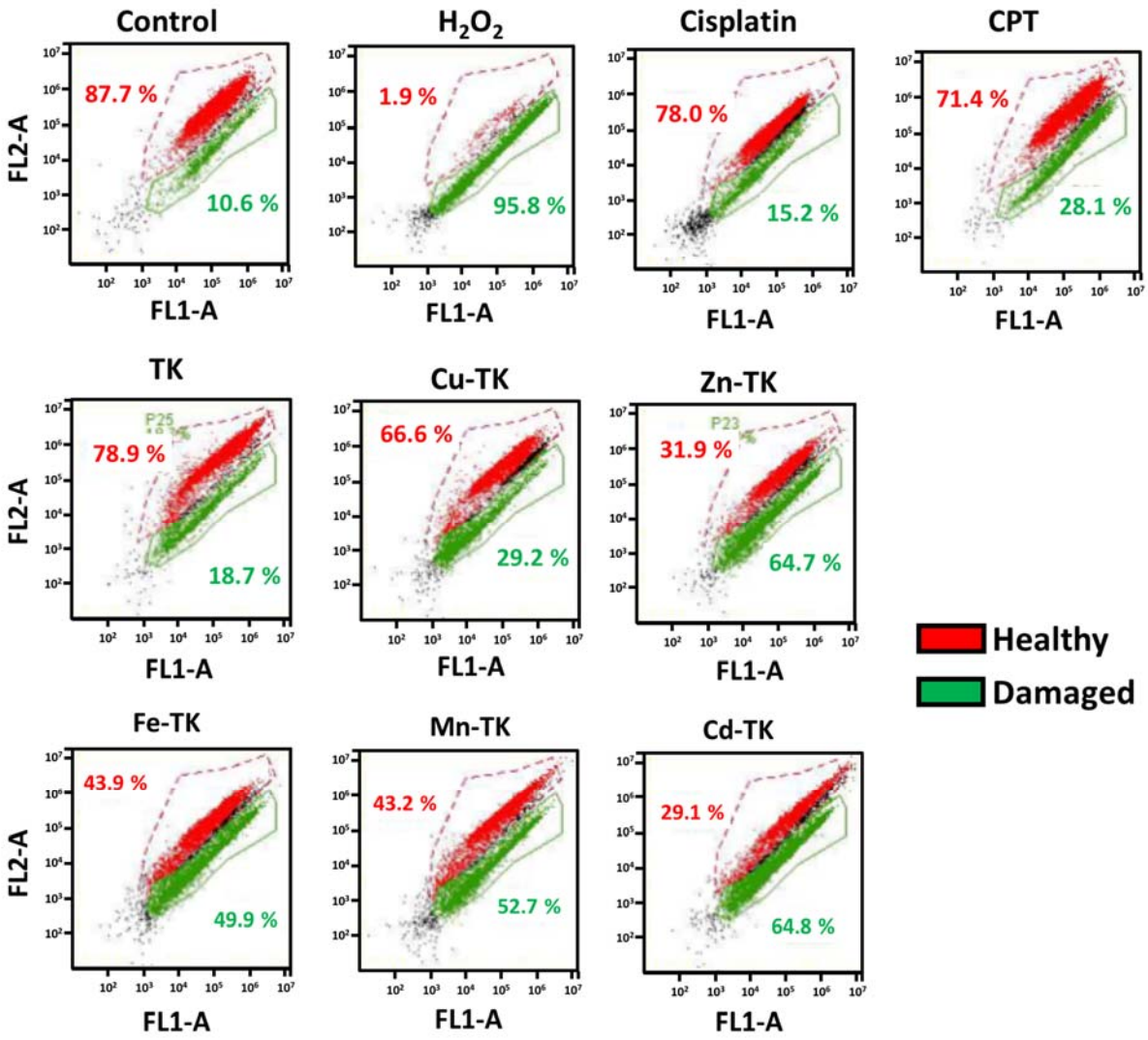


**Figure S19. M-TKs trigger the generation of high level of ROS in HeLa cells.** ROS level measurements by flow cytometry. Mitochondrial membrane potential ($\Delta\Psi m$) alterations in HeLa cells after 1 h exposure to no additives (control), CPT, Cisplatin, TK, Cu-TK, Zn-TK, Fe-TK, Mn-TK and Cd-TK (10 μM), measured using the JC-1 probe. $H_2O_2$ was used as a positive control. The experiment was performed in triplicate.

14. Migration study Inhibition of migration and invasion by wound healing assay.

The ability of the Metal-TKs to inhibit cancer cell migration was evaluated by performing scratch wound healing assay, a “wound gap” in a cell monolayer is created by scratching, and the “healing” of this gap by cell migration and growth towards the center of the gap was monitored and quantitated.[10, 11] Factors that alter the motility and/or growth of the cells can lead to increased or decreased rate of “healing” of the gap.

HeLa cells were seeded in 6-well plates with complete DMEM until a cell monolayer was formed. The cell monolayer was wounded using a plastic pipette tip. HeLa cells were then rinsed with PBS and treated with test compounds (2.5 μM) for 24 h. The wound closure was observed and imaged using an optical microscope (DMI6000, Leica).

The wound in control cells was completely recovered with cells after 24 hours as well TK-treated cells. Cells treated with Metal-TKs, CPT and cisplatin exhibited less migration after 24 hours of incubation. Effective reduction in the migration of HeLa cells (61 % less migration than in the control) was observed in group treated with Cu-TK and Cd-TK. The scratch assay findings suggest that TKs have the ability to inhibit the migration of HeLa cells.

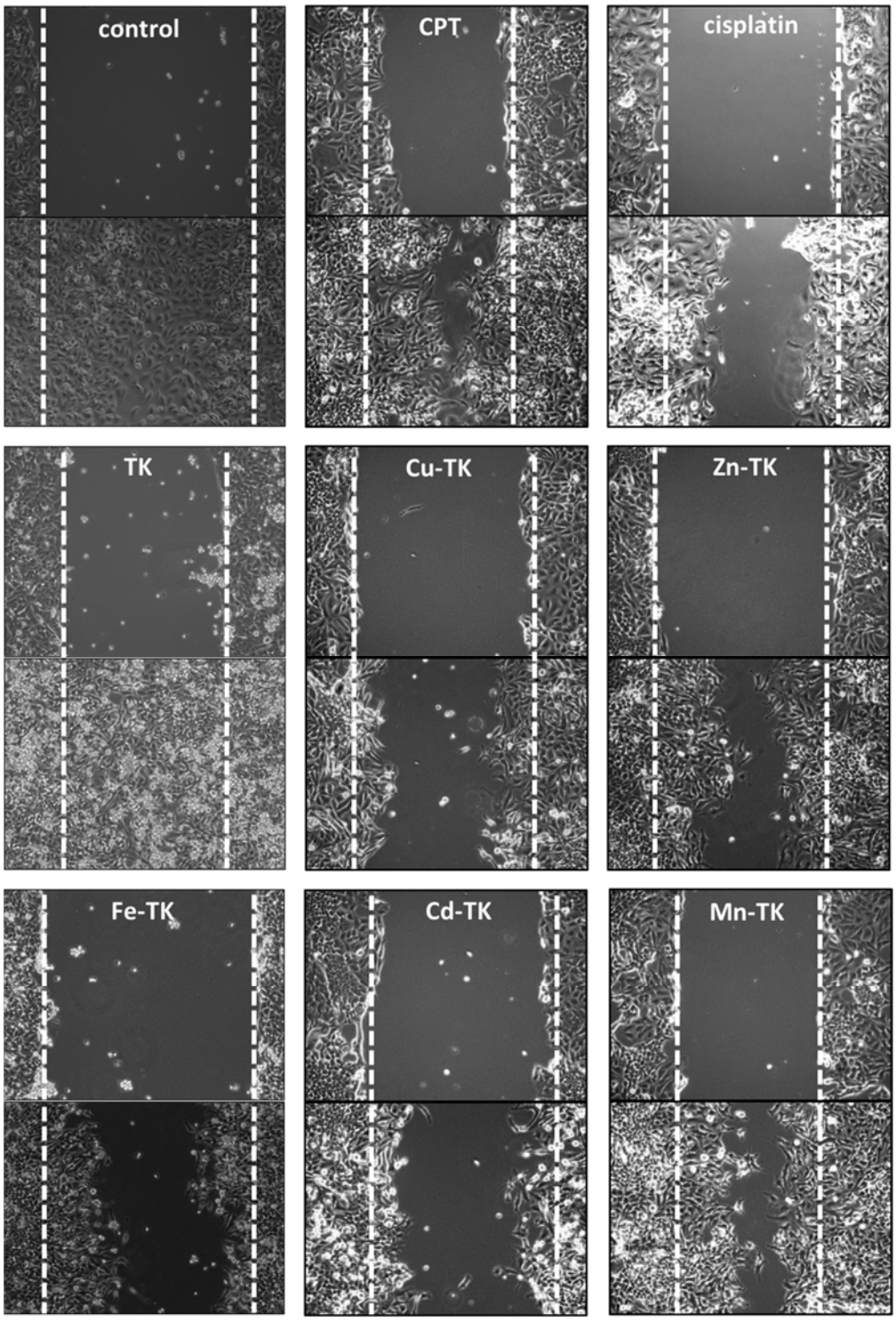


**Figure S20. M-TKs inhibit the ability of HeLa cells to migrate.** Phase-contrast images of wounded HeLa cell monolayers at two time intervals (0 and 24 h) (10 x magnification) to assess the effects on cell migration. Confluent monolayers of HeLa cells were wounded by scratching and treated with no additive (control), CPT, Cisplatin, TK, Cu-TK, Zn-TK, Fe-TK, Mn-TK and Cd-TK (2.5 μM). The experiment was performed in triplicate.

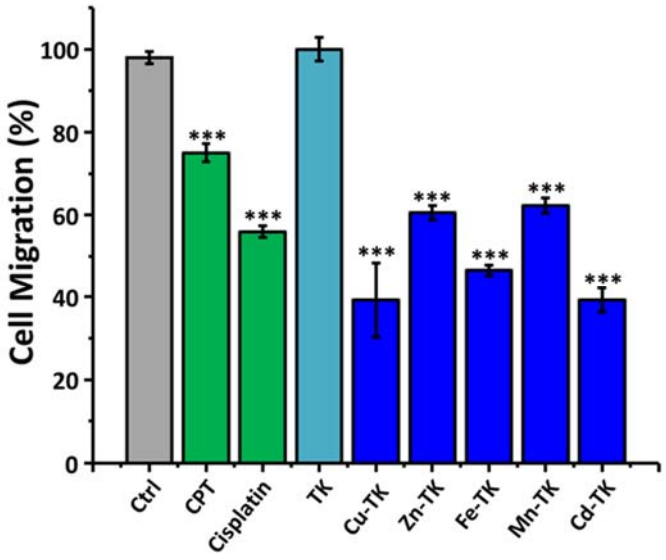


**Figure 21. Quantitative measurement of migration inhibition rate.** Scratch closure rates were analyzed quantitatively as the difference between scratch width at 0, and 24 hours and results were expressed as the percentage of cell migration. Error bars represent standard deviations of triplicate measurements. Each experiment was repeated three times with each compound. All values are expressed as mean ± STD. ($n = 3$). *$P < 0.05$, **$P < 0.01$ and ***$P < 0.001$ compared to the control.

15. Adhesion study

We determined the effects of Metal-TKs on adhesion of HeLa cells. Cells were treated with Metal-TKs for 2 h, harvested and then allowed to adhere in a new plate for 1 h. Cells were considered as adhered if they became flattened.

HeLa cells were seeded in 6-well plates into complete DMEM and incubated for 24 h. Cells were then treated with test compounds (5 μM) for 2 h. Cells were harvested and added to a new plate to adhere for 1 h. Non-adherent cells were washed off the plate, and the remaining adherent cells were counted and imaged using an optical microscope (DMI6000, Leica). Each

experiment was repeated three times with each compound. All values are expressed as mean ± STD. (n = 3). *P < 0.05, **P < 0.01 and ***P < 0.001 compared to the control.

Control group cells presented a high number of cells attached. Cisplatin and CPT showed a weak effect on the inhibition of the cell adhesion, with 91 % and 79 % of the cells been adherent. TK-treated cells showed no differences with control cells. However, the number of adhered cells was drastically reduced after Metal-TK exposition. Less flatten cells and more round cells were observed in Metal-TK group. The results indicated that TKs inhibited cell adhesion significantly.

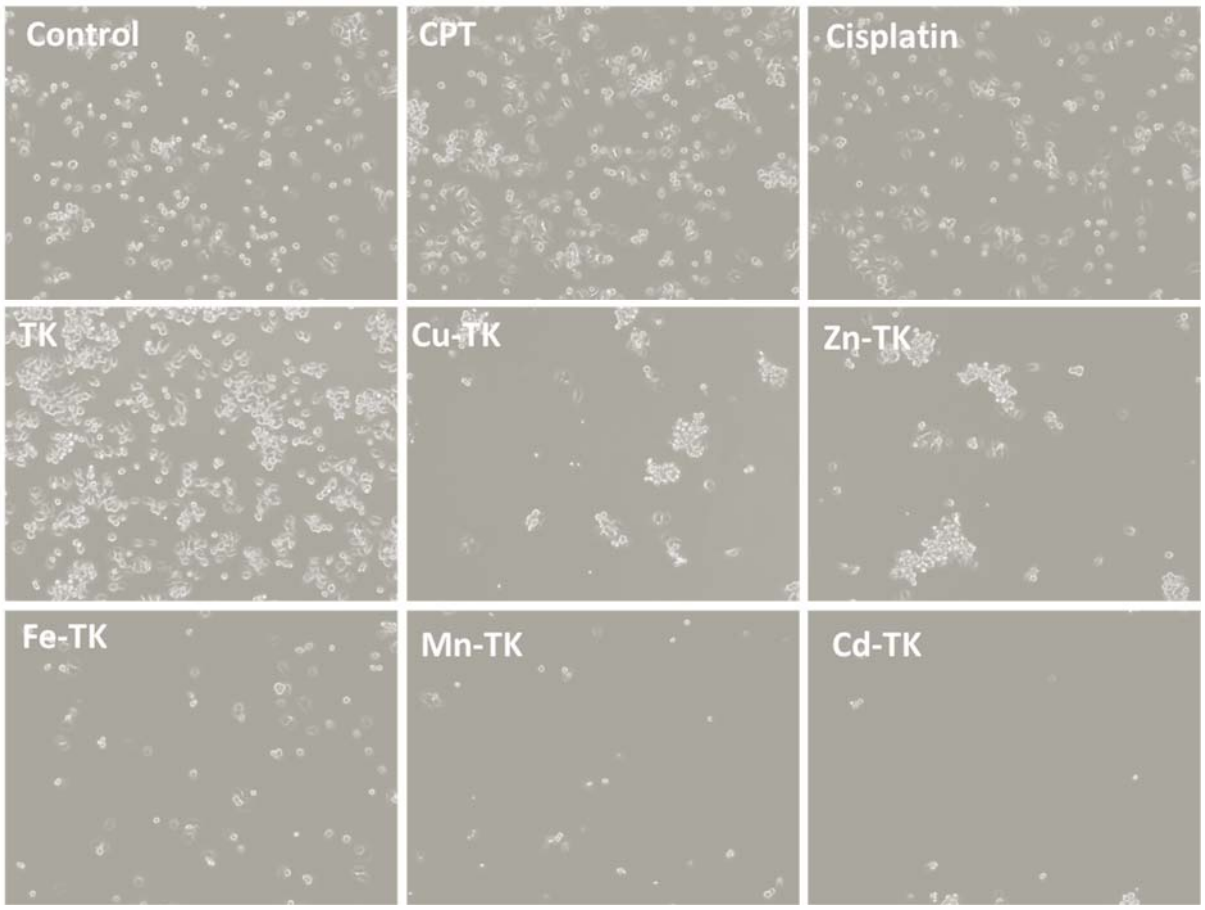


**Figure S22. M-TKs inhibit HeLa cells adhesion.** Phase-contrast images of HeLa cells after treatment, harvesting and 1 hour after reseeding into a new flask to assess the Effect on cell adhesion. HeLa cells were treated with no additive (control), CPT, Cisplatin, TK, Cu-TK, Zn-TK, Fe-TK, Mn-TK and Cd-TK (5 μM) for 2 hours, cells were then harvested and their ability to reattach to a culture dish was assessed. (10 x magnification). The experiment was performed in triplicate.

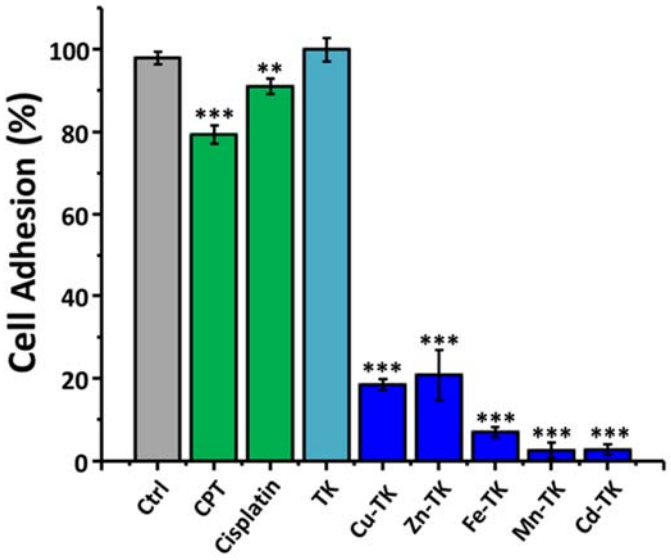


**Figure 23. Quantitative measurement of adhesion inhibition rate.** The number of cells attached after harvesting within an hour was quantified compared to control. Error bars represent standard deviations of triplicate measurements. Each experiment was repeated three times with each compound. All values are expressed as mean ± STD. (n = 3). *P < 0.05, **P < 0.01 and ***P < 0.001 compared to the control.

16. Zebrafish embryo studies

All fish were raised in accordance with the policies of the New York University Institutional Animal Care and Use Committee (IACUC) on a 14:10 h light:dark cycle at 28°C.

16.1. Embryos handling.

Embryos were exposed to all compounds in concentrations ranging from 1-10 μM and the effect on viability and cell death were assessed. Embryos were collected shortly after fertilization by natural spawning of wild-type (AB, TAB14 or TAB5) adults maintained under standard aquaculture conditions. Fertilized eggs were at 28 °C until 90 % epiboly (9 hours post fertilization (hpf). Treatment was done after this stage in order to avoid any effect on gastrulation due to metal toxicity. Embryos were analyzed at 24 hpf and scored for mortality. For survival analysis, the embryos remained in the drug solution for the duration of study and

counted for live/dead at 24, 48, 96 and 120 hpf. All data was plotted using PRISM software. All animal experimentation was approved by the Institutional Animal Care and Use Committee of NYUAD.

16.2. Cell Death Assays

Embryos surviving TK exposure to 24 hpf were dechorionated and incubated for 30 minutes in Acridine orange solution (10 mg/ml) diluted with egg water to a final concentration of 5 µg/ml. The embryos were washed at least 5 times and then mounted on glass slides with 3 % methyl cellulose for acquiring images. Imaging was carried out using the Nikon stereo-microscopes.

Terminal deoxynucleotidyl transferase dUTP nick end labeling (TUNEL) staining was carried out on fixed embryos using the Roche *In Situ* Cell Death Detection Kit with Fluorescein. Embryos were fixed in 4 % paraformaldehyde overnight. After washing in 1X PBS, the embryos were gradually dehydrated to 100 % Methanol and incubated in it for 2 hours. The embryos were gradually rehydrated back to 1X PBS and washed in 1X PBST (1X PBS with 0.1% TritonX). Embryos were permeabilized for 30 minutes in a 1X PBS solution containing 0.1% Sodium Citrate, 0.1% TritonX and 20 µg/ml Proteinase K. Following permeabilization, embryos were washed with 1X PBS and fixed again with 4% PFA for 10 minutes. After washing the embryos again with 1X PBS, de-yolked embryos were incubated in 10 µL of TUNEL solution (1 µl TUNEL TdT enzyme + 9 µl Labeling Mix) for 1hour in the dark at 37 °C. After washing with 1X PBST, the embryos were mounted in 3% methyl cellulose and imaged on the Nikon stereo-microscopes. The imaged embryos were analyzed using Nikon NIS-Elements Object Count. The numbers of TUNEL positive cells were obtained at a selected tail region of the embryo and plotted using PRISM.

## References


1. T. Prakasam, M. Lusi, M. Elhabiri, C. Platas-Iglesias, J.-C. Olsen, Z. Asfari, S. Cianférani-Sanglier, F. Debaene, L. J. Charbonnière and A. Trabolsi, *Angew. Chem. Int.*, 2013, **52**, 9956-9960.
2. T. Prakasam, R. A. Bilbeisi, M. Lusi, J.-C. Olsen, C. Platas-Iglesias and A. Trabolsi, *Chem. Commun.*, 2016, **52**, 7398-7401.
3. R. A. Bilbeisi, T. Prakasam, M. Lusi, M. Elhabiri, C. Platas-Iglesias, J. C. Olsen, L. J. Charbonniere and A. Trabolsi, *Chem.Sci*, 2015, **7**, 2524-2531.
4. H. E. Gottlieb, V. Kotlyar and A. Nudelman, *J. Org. Chem.*, 1997, **62**, 7512-7515.
5. G. R. Fulmer, A. J. Miller, N. H. Sherden, H. E. Gottlieb, A. Nudelman, B. M. Stoltz, J. E. Bercaw and K. I. Goldberg, *Organometallics*, 2010, **29**, 2176-2179.
6. M. Kajstura, H. D. Halicka, J. Pryjma and Z. Darzynkiewicz, *Cytometry A*, 2007, **71**, 125-131.
7. H. H. Grunicke, *Eur. J. Cancer Clin. Oncol.*, **27**, 281-284.
8. R. J. Boohaker, M. W. Lee, P. Vishnubhotla, J. M. Perez and A. R. Khaled, *Current medicinal chemistry*, 2012, **19**, 3794-3804.
9. S. Alarifi, D. Ali, S. Alkahtani, A. Verma, M. Ahamed, M. Ahmed and H. A. Alhadlaq, *Int. J. Nanomed.*, 2013, **8**, 983-993.
10. N. N. Nissen, P. J. Polverini, A. E. Koch, M. V. Volin, R. L. Gamelli and L. A. DiPietro, *Am. J. Pathol.*, 1998, **152**, 1445-1452.
11. J. E. N. Jonkman, J. A. Cathcart, F. Xu, M. E. Bartolini, J. E. Amon, K. M. Stevens and P. Colarusso, *Cell Adhes. Migr.*, 2014, **8**, 440-451.